

Decomposition of the Wave Manifold into Lax Admissible Regions and its Application to the Solution of Riemann Problems

Cesar S. Eschenazi^{*1}, Wanderson J. Lambert^{†2}, Marlon M. López-Flores^{‡3}, Dan Marchesin^{§4}, and Carlos F.B. Palmeira^{¶5}

¹*Universidade Federal de Minas Gerais – UFMG, Belo Horizonte, MG, CEP: 31270-901*

²*Universidade Federal de Alfenas – UNIFAL, Alfenas, MG, CEP: 37130-001*

³*Instituto Nacional de Matemática Pura e Aplicada – IMPA, Rio de Janeiro, RJ, Brazil, CEP: 22460-320*

⁴*Instituto Nacional de Matemática Pura e Aplicada – IMPA, Rio de Janeiro, RJ, Brazil, CEP: 22460-320*

⁵*Pontifícia Universidade Católica do Rio de Janeiro – PUC-Rio, Rio de Janeiro, RJ - Brasil, CEP: 22451-900*

Abstract

We utilize a three-dimensional manifold to solve Riemann Problems that arise from a system of two conservation laws with quadratic flux functions. Points in this manifold represent potential shock waves, hence its name wave manifold. This manifold is subdivided into regions according to the Lax admissibility inequalities for shocks. Finally, we present solutions for the Riemann Problems for various cases and exhibit continuity relative to L and R data, despite the fact that the system is not strictly hyperbolic. The usage of this manifold regularizes the solutions despite the presence of an elliptic region.

Contents

1	Introduction	2
2	The Wave Manifold and Hugoniot Curves	4
2.1	New Coordinates	6
3	Characterizing \mathcal{C}_s and \mathcal{C}_f	8
4	Decomposition of the Wave Manifold	9
5	Finding Son'_s and Son'_f	13
6	Lax’s Shocks in \mathcal{W}	14

^{*}email: cseschenazi@gmail.com
[†]email: wanderson.lambert@unifal-mg.edu.br
[‡]email: mmlf@impa.br
[§]email: marchesin@impa.br
[¶]email: fredpalm@gmail.com - Corresponding author.

7	Rarefactions and Composites	16
7.1	Rarefactions	16
7.2	Composites	18
8	Wave Curves	20
8.1	Local Wave Curves	20
8.2	Decomposing C_s according to wave curves structures	21
9	Riemann Solution	22
9.1	The wave curves in each region	23
9.2	The wave curves on the plane uv	24
9.3	The saturated surfaces	25
9.4	2-reverse wave sequence	27
9.5	Examples of solutions	28
9.6	The Regions in Phase Space	36
1	Characterizing the L2 Condition	39
2	Lax's inequalities in the wave manifold	40
3	Choices	41
3.1	Choice 1	41
3.2	Choice 2	41

1 Introduction

We consider the system of two partial differential equations

$$W_t + F(W)_x = 0, \tag{1.1}$$

with initial conditions

$$W(x, t = 0) = \begin{cases} W_L & \text{if } x < 0, \\ W_R & \text{if } x > 0. \end{cases} \tag{1.2}$$

We will take $W = (u, v) \in \mathbb{R}^2$ and F a map $F : \mathbb{R}^2 \rightarrow \mathbb{R}^2$, the two components of which are called *flux functions*. Equation (1.1) appears in fluid dynamics and together with initial conditions (1.2) is called a Riemann problem.

We are mainly interested in the so called shock solutions, defined by

$$W = \begin{cases} W & \text{for } x < st, \\ W' & \text{for } x > st, \end{cases}$$

where s is the shock propagation speed, $W = (u, v)$ and $W' = (u', v')$ are the states to be connected by the shock.

In order to have physical meaning as a shock, the speed and the states must satisfy the so called *Rankine-Hugoniot* condition [10].

$$F(W) - F(W') = s(W - W'), \quad (1.3)$$

for some s . This leads to the definition of Hugoniot curve associated to a given state $W = (u_0, v_0)$, in Section 2.

Furthermore, not all arcs of Hugoniot curves are useful to construct solutions. Shock curve arcs must satisfy some extra conditions called admissibility conditions. In [1], Liu's admissibility entropy criterion was introduced within the wave manifold context. There it was shown that under certain extra assumptions, which will be considered in the current paper, Liu's entropy criterion can be replaced by the Lax entropy inequality conditions. These inequalities relate s and the eigenvalues of $DF(u, v)$. Hugoniot arc curves satisfying these inequalities are called *shock curve arcs* or *admissible arcs*.

We adopt here the topological point of view, as described in [5]. We consider the space \mathbb{R}^5 of coordinates (u, v, u', v', s) and in it the three-dimensional manifold defined by $F(u, v) - F(u', v') - s(u - u', v - v') = 0$. In this manifold, we consider the curves defined by (u, v) constant, called Hugoniot curves, their projections onto the state space are the classical Rankine-Hugoniot curves, see [1]. This manifold is called *wave manifold*.

In a series of papers (see [1, 3, 7, 8]), this manifold and its Hugoniot curves have been studied for the case where F is a polynomial of degree two. The wave manifold has been characterized, relevant surfaces (*characteristic*, *sonic* and *sonic'*) have been defined, the intersection of Hugoniot curves with these surfaces has been studied, and the Lax inequalities have been interpreted in this context. Here, also considering F as a polynomial of degree two, we decompose the *characteristic* and *sonic'* surfaces in their fast and slow components. And also decompose the wave manifold in regions which we call admissible or non-admissible regions.

As stated at the beginning of Section 2, we will restrict ourselves to the symmetric Case IV of the Sheaffer-Shearer classification, see [9]. A study of cases I, II, III and IV (non symmetric case) can be found in [6].

We will also consider rarefaction and composite solutions, to be defined in Section 7 and used in Sections 8 and 9.

This paper is organized as follows: In Section 2, we review some basic facts and definitions, introduce new variables and describe the *characteristic*, *sonic* and *sonic'* surfaces, [5]. In Section 3, we characterize the slow and fast components of the characteristic surface associated with the eigenvalues of DF . We also characterize the *coincidence curve*, which is the boundary of these two components. In Section 4, we describe how the *characteristic*, *sonic* and *sonic'* surfaces divide the wave manifold into twelve regions and characterize the surface formed by the Hugoniot curves through points of the *coincidence curve*. This surface will be called *saturated of the coincidence curve by Hugoniot curves* and denoted by *SSC*. It is tangent to the *characteristic* and *sonic'* surfaces. In Section 5, we characterize the slow and fast components of the *sonic'* surface, associated with the slow shock speed and the fast shock speed. We show that the boundaries of these two components are a straight line and the *hysteresis' curve*, which is the curve where Hugoniot curves are tangent to the *sonic'* surface. In Section 6, we identify some of regions in the wave manifold where Lax's inequalities are satisfied, indicating in which regions there are local shock curve arcs and in which of these regions there are nonlocal shock curve arcs.

In Section 7, we present the rarefaction and composite curves, derived from the rarefaction solutions mentioned before, and decompose the state space ((u, v) -plane) in elliptic and hyperbolic regions. In Section

8, we introduce the wave curve in the wave manifold, such curves consist of arcs of admissible Hugoniot curves, rarefaction curves and composite curves of the same family. In Section 9, we use all the elements previously defined to solve Riemann problems.

It is known from [3] that a Hugoniot curve through points of the secondary bifurcation has two components, a straight line and a curve. The lines generate a plane and the curves a surface, which we will call *saturated of secondary bifurcation by Hugoniot curves*, denoted by *SSB*. In Appendix 1, we characterize the regions of the wave manifold where condition **L2**, introduced in Section 6, is satisfied. In Appendix 3, we justify the choices of the flux function, parameters and coordinates used in this paper.

2 The Wave Manifold and Hugoniot Curves

In this section, we review some basic facts and definitions and introduce new variables. We will define the *characteristic*, *sonic* and *sonic'* surfaces, since they will appear as boundaries of the admissible regions.

We refer the reader to Section 2 of [3] for basic definitions. For the sake of completeness, we briefly present some necessary concepts needed here.

We consider the equation (1.1) with F given by $F = (f, g)$, where

$$\begin{cases} f(u, v) = v^2/2 + (b_1 + 1)u^2/2 + a_1u + a_2v, \\ g(u, v) = uv + a_3u + a_4v, \end{cases} \quad (2.1)$$

for $b_1 > 1$. This is the symmetric Case IV in the Schaeffer and Shearer classification, see [9].

Given a point $W = (u, v)$, in the (usually called) “state space”, *the Hugoniot curve through this point is defined as the set of points $W' = (u', v')$, such that there exists s such that satisfies $F(W) - F(W') = s(W - W')$* . We clearly see that this curve passes through W .

To study Hugoniot curves, we consider $\mathbb{R}^5 = \{(u, v, u', v', s)\}$ and in it the three-dimensional manifold defined by $F(W) - F(W') = s(W - W')$. Since this manifold is singular along the diagonal $W = W'$, along this diagonal, we perform a blow up, which, in this simple case, is obtained using the coordinate transformations given by $U = (u + u')/2$, $V = (v + v')/2$, $X = u - u'$, $Y = v - v'$, and $Z = Y/X$ and factoring X^2 . We also set $c = a_3 - a_2 > 0$. Using these new coordinates, we get

$$(1 - Z^2)(V + a_2) - Z(b_1U + a_1 - a_4) + c = 0 \quad \text{and} \quad Y = ZX.$$

The two above equations define a regular three-dimensional manifold, which will be referred as the *wave manifold* and will be denoted by \mathcal{W} .

Since Z is a direction, we may think of the wave manifold \mathcal{W} , as contained in $\mathbb{R}^4 \times \mathbb{R}P^1$, or, which is the same as, $\mathbb{R}^4 \times S^1$. These coordinates are not valid at $Z = \infty$, but there are no special features at infinity, so, we can just use X, U, V, Z to study Hugoniot curves.

Defining $\tilde{U} = b_1U + a_1 - a_4$ and $\tilde{V} = V + a_2$ we obtain the equation $G_1 = (1 - Z^2)\tilde{V} - Z\tilde{U} + c = 0$, used in ([7, 3, 4]).

Hugoniot curves in the wave manifold are defined by $u = \text{constant}$ and $v = \text{constant}$, which, in these new coordinates, become

$$\begin{cases} 2\tilde{U} + b_1X = 2b_1u_0 + 2(a_1 - a_4), \\ 2\tilde{V} + ZX = 2v_0 + 2a_2. \end{cases} \quad (2.2)$$

As shown in [7], Hugoniot curves are connected and foliate \mathcal{W} except along a straight line B , contained on the plane, Π , defined by $Z = 0$. The straight line B is called *secondary bifurcation*. Hugoniot curves through points in B are formed by two arcs: a straight line *hugl* and a curve *hugc*. These two arcs intersect at a point of B . The lines *hugl* fill the plane Π .

Definition 1. *The set of Hugoniot curves through points of $hugc$ is called saturated of the secondary bifurcation by Hugoniot curves and denoted by SSB .*

It is easy to see that SSB is a two-dimensional sub-manifold of \mathcal{W} and that SSB and Π intersect transversely along B .

The same conclusions are valid for Hugoniot' curves, defined by $u' = constant$ and $v' = constant$. Hugoniot' curves are connected and foliate \mathcal{W} except along a straight line B' , also contained on the plane Π . Hugoniot' curves through points in B' are formed by two arcs: a straight line *hugl'* and a curve *hugc'*. These two arcs intersect at a point of B' . The lines *hugl'* also fill the plane Π . In a similar way the curves *hugc'* form a two-dimensional sub-manifold called *saturated of the secondary bifurcation by Hugoniot' curves*, denoted by SSB' . The plane Π and intersect transversely along B' .

There are three important surfaces in the study of the wave manifold: Characteristic (denoted by \mathcal{C}), Sonic (denoted by Son) and Sonic' (denoted by Son').

To define Son and Son' , one must look at the speed s as a real function in \mathcal{W} given by $[f(u, v) - f(u', v')]/(u - u')$ or $[g(u, v) - g(u', v')]/(v - v')$. Using coordinates X , \tilde{U} and \tilde{V} , we have

$$s = \frac{\tilde{U}}{b_1} + \frac{\tilde{V}}{Z}, \quad (2.3)$$

To define Son , we restrict s to a Hugoniot curve, and look at its critical points. The set of these critical points for all Hugoniot curves is the *Sonic surface*, Son . In the same way, we define the *Sonic' surface*, Son' , as the set of all critical points of s restricted to a Hugoniot' curve. This was done in [7], obtaining equations

$$2[Z^2 + b_1 + 1]\tilde{U} + 2[Z^3 + (b_1 + 3)Z]\tilde{V} - [Z^2 - (b_1 + 1)]X = 0 \quad (2.4)$$

for Son and

$$2[Z^2 + b_1 + 1]\tilde{U} + 2[Z^3 + (b_1 + 3)Z]\tilde{V} + [Z^2 - (b_1 + 1)]X = 0 \quad (2.5)$$

for Son' .

We list some important known facts about \mathcal{C} , Son and Son' , for the quadratic flux functions considered here.

Fact 1.- \mathcal{C} is topologically a cylinder.

Fact 2.- Given a Hugoniot curve, either it intersects \mathcal{C} transversely in two points, or it is tangent or it does not intersect \mathcal{C} .

Fact 3.- The above mentioned set of tangency points form a simple closed curve. This curve does not bound a disk in \mathcal{C} and divides it into two components, denoted by \mathcal{C}_s and \mathcal{C}_f . This simple closed curve is called *coincidence curve in \mathcal{C}* , denoted by $\mathcal{E}_{\mathcal{C}}$.

Fact 4.- Any Hugoniot curve through a point \mathcal{U} , $sh(\mathcal{U})$, which intersects \mathcal{C} transversely, does it at a point $\mathcal{U}_s = sh(\mathcal{U}) \cap \mathcal{C}_s$ and in another point $\mathcal{U}_f = sh(\mathcal{U}) \cap \mathcal{C}_f$. The value of the speed s in \mathcal{U}_s is smaller

than the value of s in \mathcal{U}_f . Proof of this fact will be presented in Section 3, where we will characterize \mathcal{C}_s and \mathcal{C}_f .

Fact 5.- Son and Son' are topologically Möbius band and they intersect \mathcal{C} along a curve called *inflection locus*, denoted by \mathcal{I} , which is diffeomorphic to \mathbb{R} , and contains the intersection point of B and \mathcal{C} . They also intersect along two straight lines, each of which intersects transversally \mathcal{C} at a point of the inflection locus.

Fact 6.- Generically, a Hugoniot curve through a point \mathcal{U} , $sh(\mathcal{U})$, intersects Son' in 0, 2 or 4 points. If $sh(\mathcal{U}) \cap Son'$ has 2 points, then s has the same value in these 2 points as the value of s either in \mathcal{U}_s or in \mathcal{U}_f . In the first case, the points are said to be in Son'_s and in the second case, in Son'_f . If the intersection has 4 points, then s has the same value of s in \mathcal{U}_s in two of them and the value of s in \mathcal{U}_f in the other two. The first two are points in Son'_s and the other two in Son'_f .

2.1 New Coordinates

In this paper, we use coordinates $z = 1/Z$, t and Y . The main advantage is that they are valid for $\mathcal{W} - \Pi$ and Π becomes the plane $z = \infty$. To define t , we start by writing the equation of \mathcal{W} in term of the variables \tilde{U} , $V_1 = V + a_3 = \tilde{V} + c$ and z . We get $G = 0$, where $G = (z^2 - 1)V_1 - z\tilde{U} + c$. The parameter t is defined by

$$\tilde{U} = \frac{2cz}{z^2 + 1} + ct(z^2 - 1) \quad \text{and} \quad V_1 = \frac{c}{z^2 + 1} + ctz. \quad (2.6)$$

For each fixed z , the parameter t measures as far as \tilde{U} and V_1 are away from the coincidence curve in \mathcal{C} in the orthogonal direction to it.

In these new coordinates, the characteristic surface, \mathcal{C} , is the plane $Y = 0$. The *sonic* and the *sonic'* surfaces are given by the equations obtained from equations (2.4) and (2.5) by transforming from variables \tilde{U} , \tilde{V} , X and Z to the new coordinates z , t and Y . We obtain $son = 0$, where

$$son = -2c[(b_1 + 1)z^5 + (b_1 + 4)z^3 + 3z]t - [(b_1 + 1)z^4 + b_1z^2 - 1]Y - 2c[(b_1 - 1)z^2 + 1], \quad (2.7)$$

and $son' = 0$, where

$$son' = -2c[(b_1 + 1)z^5 + (b_1 + 4)z^3 + 3z]t + [(b_1 + 1)z^4 + b_1z^2 - 1]Y - 2c[(b_1 - 1)z^2 + 1]. \quad (2.8)$$

The shock speed, s , is written as

$$s = \frac{c[(b_1 + 1)tz^4 + b_1z^2t + (b_1 + 2)z - t]}{b_1(z^2 + 1)}. \quad (2.9)$$

Parametric equations for Hugoniot curves in z , t , Y coordinates are obtained by replacing \tilde{U} , \tilde{V} and X into equations in (2.2), by their values in terms of z , t , Y and solving the system with respect to t and Y . We get:

$$\begin{cases} z = z, \\ t = \frac{(v_0 + a_3)b_1z^3 + (b_1u_0 + a_1 - a_4)z^2 - [b_1(v_0 + a_2) + 2c]z + b_1u_0 + a_1 - a_4}{c(z^2 + 1)[(b_1 - 1)z^2 + 1]}, \\ Y = \frac{-2(v_0 + a_3)z^2 + 2(b_1u_0 + a_1 - a_4)z + 2(v_0 + a_2)}{(b_1 - 1)z^2 + 1}. \end{cases} \quad (2.10)$$

From the expression of Y in (2.10), we see that a Hugoniot curve intersects \mathcal{C} depending on whether $\mathcal{E}_{ss} = (b_1 u_0 + a_1 - a_4)^2 + 4(v_0 + a_3)(v_0 + a_2)$ is positive or negative: It intersects \mathcal{C} in two points if $\mathcal{E}_{ss} > 0$ and does not intersect \mathcal{C} if $\mathcal{E}_{ss} < 0$.

Definition 2. *The curve $\mathcal{E}_{ss} = 0$ is called coincidence curve in the state space, it is an ellipse. Its interior is called elliptic region and its exterior is called hyperbolic region.*

As we shall see in Subsection 7.1, there are no rarefaction curves through points of the elliptic region and through every point of the hyperbolic region pass two transversal rarefaction curves.

Parametric equations for Hugoniot' curves are obtained from equations (2.10) by interchanging Y with $-Y$.

Substituting the second equation of (2.10) into equation (2.9), we get the expression of the shock speed $s = s(u_0, v_0, z)$ along a Hugoniot curve.

In order to get the expression of a Hugoniot curve through a given point (z_0, t_0, Y_0) , we start by solving system (2.10) in terms of u_0 and v_0 obtaining

$$\begin{cases} u_0(z, t, Y) = \frac{b_1 z(z^2 + 1)Y + 2c(z^4 - 1)t - 2(a_1 - a_4)z^2 + 4cz - 2(a_1 - a_4)}{2b_1(z^2 + 1)}, \\ v_0(z, t, Y) = \frac{(z^2 + 1)Y + 2cz(z^2 + 1)t - 2a_2(z^2 + 1) - 2cz^2}{2(z^2 + 1)}. \end{cases} \quad (2.11)$$

Substituting $u_0(z_0, t_0, Y_0)$ and $v_0(z_0, t_0, Y_0)$ from (2.11) into equation (2.10), we get the parametric equations for the Hugoniot curve through a point (z_0, t_0, Y_0) ,

$$\begin{cases} z = z, \\ t = \frac{Dz^3 + Ez^2 + Fz + G}{c(z_0^2 + 1)[(b_1 - 1)z^4 + b_1 z^2 + 1]}, \\ Y = \frac{Az^2 + Bz + C}{(z_0^2 + 1)[(b_1 - 1)z^2 + 1]}. \end{cases} \quad (2.12)$$

where

$$\begin{aligned} A &= -[2c + 2ct_0 z_0(1 + z_0^2) + Y_0(z_0^2 + 1)], \\ B &= 4cz_0 + 2ct_0(z_0^4 - 1) + b_1 Y_0 z_0(z_0^2 + 1), \\ C &= -2cz_0^2 + 2ct_0 z_0(1 + z_0^2) + Y_0(z_0^2 + 1), \\ D &= 2cb_1 + 2cb_1 t_0 z_0(z_0^2 + 1) + b_1 Y_0(z_0^2 + 1), \\ E &= 2ct_0(1 - z_0^4) - b_1 z_0 Y_0(z_0^2 + 1) - 4cz_0, \\ F &= 4c(z_0^2 + 1) + 2cb_1 t_0 z_0(1 + z_0^2) + b_1 Y_0(z_0^2 + 1) - 2cb_1 z_0^2, \\ G &= -4cz_0 + 2ct_0(1 - z_0^4) - b_1 z_0 Y_0(1 + z_0^2). \end{aligned}$$

It is clear from the above expressions that, given a point $(z_0, t_0, Y_0) \in \mathcal{W}$, its Hugoniot curve will intersect \mathcal{C} or not, depending on whether $B^2 - 4AC$ is positive or negative. If $B^2 - 4AC = 0$, the Hugoniot curve will be tangent to \mathcal{C} along the *coincidence curve in \mathcal{C}* , denoted by $\mathcal{E}_{\mathcal{C}}$. Let us see that in these new coordinates the coincidence curve in \mathcal{C} is given simply by $t = 0$, and, of course, $Y = 0$. Straightforward computation shows that for $Y = 0$, $B^2 - 4AC = 4c^2 t_0^2 (1 + z_0^2)^4$, and also computing dY/dz from (2.12) and setting

$t_0 = 0, Y_0 = 0$, we get 0, which shows that along the curve $Y = 0, t = 0$. The Hugoniot curves are tangent to the characteristic surface (the plane $Y = 0$ in these coordinates). So, the line $(z, t = 0, Y = 0)$, is the coincidence curve in \mathcal{C} . Let us call \mathcal{C}_s the $t < 0$ region and \mathcal{C}_f the $t > 0$ region.

3 Characterizing \mathcal{C}_s and \mathcal{C}_f

As we will see in Section 6, shock curve arcs will either start on \mathcal{C}_s or on Son'_s . So we must characterize \mathcal{C}_s and \mathcal{C}_f . In Section 5, we will define and characterize Son'_s and Son'_f .

The speed s along a Hugoniot curve through a point (z_0, t_0, Y_0) is obtained by substituting $u_0(z_0, t_0, Y_0)$ and $v_0(z_0, t_0, Y_0)$ into the expression $s = s(u_0, v_0, z)$ giving

$$s_{hug} = \frac{s_{p3}z^3 - s_{p2}z^2 - s_{p1}z + s_{p0}}{2b_1(z_0^2 + 1)[(b_1 - 1)z^2 + 1]}, \quad (3.1)$$

where

$$\begin{aligned} s_{p3} &= b_1(b_1 + 1) \left\{ Y_0(z_0^2 + 1) + 2c[1 + z_0 t_0(z_0^2 + 1)] \right\}, \\ s_{p2} &= (b_1 + 1)[b_1 z_0 Y_0(z_0^2 + 1) + 2c(2z_0 + t_0 z_0^4 - t_0)], \\ s_{p1} &= b_1 \left\{ Y_0(z_0^2 + 1) + 2c[z_0 t_0(z_0^2 + 1) - 2z_0^2 - 1] \right\}, \\ s_{p0} &= b_1 z_0 Y_0(z_0^2 + 1) + 2c(2z_0 + t_0 z_0^4 - t_0). \end{aligned}$$

The equation of the shock speed s along a Hugoniot curve through a point $(z_0, t_0, 0)$ on the characteristic surface (characteristic speed) is obtained by substituting $Y_0 = 0$ into equation (3.1)

$$s_{ch} = \frac{s_{ch3}z^3 - s_{ch2}z^2 - s_{ch1}z + s_{ch0}}{b_1(z_0^2 + 1)[(b_1 - 1)z^2 + 1]}, \quad (3.2)$$

where

$$\begin{aligned} s_{ch3} &= b_1 c [t_0 z_0 (1 + z_0^2) + 1] (1 + b_1), \\ s_{ch2} &= c (t_0 z_0^4 + 2z_0 - t_0) (1 + b_1), \\ s_{ch1} &= b_1 c (t_0 z_0^3 - 2z_0^2 + t_0 z_0 - 1), \\ s_{ch0} &= c (t_0 z_0^4 + 2z_0 - t_0). \end{aligned}$$

Lemma 1. *If $(z_0, t_0, 0)$ and $(z_1, t_1, 0)$ are the intersections of a Hugoniot curve with \mathcal{C} , then, one of them is on \mathcal{C}_s and the other on \mathcal{C}_f . Furthermore, the value of s at the point on \mathcal{C}_s is always smaller than the value of s at the point on \mathcal{C}_f (thus the subscripts s stand for slow and f for fast).*

Proof. A Hugoniot curve through a point on the characteristic has parametric equations

$$\begin{cases} z = z, \\ t = \frac{D_0 z^3 + E_0 z^2 + F_0 z + G_0}{c(z_0^2 + 1)[(b_1 - 1)z^4 + b_1 z^2 + 1]}, \\ Y = \frac{A_0 z^2 + B_0 z + C_0}{(z_0^2 + 1)[(b_1 - 1)z^2 + 1]}. \end{cases} \quad (3.3)$$

where $A_0, B_0, C_0, D_0, E_0, F_0$ and G_0 are obtained from (2.12). It is just a matter of making $Y_0 = 0$ in equations (2.12).

Solving equation $Y = 0$ we get z_0 and $z_1 = -[t_0(1 + z_0^2) - z_0]/[t_0 z_0(1 + z_0^2) + 1]$, values of z at the intersection points with \mathcal{C} . It is easy to see that $z_0 = z_1$ if and only if $t_0 = 0$, characterizing the *coincidence curve*.

Replacing z by z_1 in the expression of t in equations (3.3), we get the expression of t_1 . A straightforward computation shows that $t_0 \cdot t_1 < 0$, so, an intersection point is on \mathcal{C}_s and the other one on \mathcal{C}_f .

Let $sch0$ and $sch1$ be the characteristic speeds for $z = z_0$ and $z = z_1$. Straightforward computations give $sch0 - sch1 = c(z_0^2 + 1)t_0$. It follows that $sch0 > sch1$ if and only if $t_0 > 0$. So, the value of s at the point on \mathcal{C}_f is larger than the value of s at the point on \mathcal{C}_s . \square

4 Decomposition of the Wave Manifold

In this section, we describe how the *characteristic, sonic* and *sonic'* surfaces divide $\mathcal{W} - \Pi$.

Recall that, here, $\mathcal{W} - \Pi$ is just the (z, t, Y) space. Let Π_z be the fixed z plane. In it, we will consider the t and Y axis inherited from the (z, t, Y) space. We will consider t to be the horizontal axis and Y to be the vertical axis.

It follows from equations (2.7) and (2.8) that Son and Son' are ruled surfaces. Their intersections with Π_z are straight lines. We will see how these intersections vary with z . The intersection $\mathcal{C} \cap \Pi_z$ is just the t -axis, *i.e.*, the line $Y = 0$.

Let $Sz = Son \cap \Pi_z$ and $S'z = Son' \cap \Pi_z$. For a fixed z , Sz and $S'z$ intersect at the point $(t = t_0, Y = 0)$, t_0 given in equation (4.1). Letting z vary, these points in \mathcal{C} are on the inflection locus curve, \mathcal{I} , whose expression is given by:

$$t = \frac{(b_1 - 1)z^2 + 1}{z[(b_1 + 1)z^4 + (b_1 + 4)z^2 + 3]}. \quad (4.1)$$

For $z = 0$, Sz and $S'z$, become horizontal lines with equations $Y = 2c$ and $Y = -2c$, respectively. Figure 1 illustrates typical relative positions of Sz and $S'z$ in the (t, Y) -plane for some fixed values of z , $z < 0$.

Besides intersecting at the inflection locus, Son and Son' intersect for

$$z_{crit_1} = \frac{1}{\sqrt{b_1 + 1}} \quad \text{and} \quad z_{crit_2} = -\frac{1}{\sqrt{b_1 + 1}}, \quad (4.2)$$

values of z that cancel out the coefficient of Y in equations (2.7) and (2.8). Straightforward computations show that for $z = z_{crit_1}$, we get $t_1 = -b_1 \sqrt{b_1 + 1}/[2(b_1 + 2)]$ and for $z = z_{crit_2}$, we get $t_2 = b_1 \sqrt{b_1 + 1}/[2(b_1 + 2)]$. So, for these values of z , Sz and $S'z$, coincide and become the vertical lines $t = t_1$ and $t = t_2$. In the wave manifold \mathcal{W} we have two straight lines $(z = z_{crit_1}, t = t_1, Y)$ and $(z = z_{crit_2}, t = t_2, Y)$.

Definition 3. *The straight lines $(z = z_{crit_1}, t = t_1, Y)$ and $(z = z_{crit_2}, t = t_2, Y)$ are called double sonic locus.*

In this way, $Son \cap Son'$ is formed by the inflection locus and the double sonic locus, [5].

Remark 1. *In papers with classical approach the double sonic locus is called double contact.*

We can state,

Proposition 1. *The characteristic, sonic and sonic' surfaces divide $\mathcal{W} - \Pi$ into twelve regions.*

Proof. It is enough to consider the half-space $Y > 0$, since a symmetric division will appear in the $Y < 0$ half-space. For each fixed z we will look at the two-dimensional regions in which the plane Π_z is divided and see how these two-dimensional regions form 3-dimensional regions as z moves. As described above, there are 3 critical values in the z movement: $z = z_{crit_2}$, $z = 0$ and $z = z_{crit_1}$. The equation of Sz is obtained by solving (2.7) for Y .

Let $(t_0, 0)$ be the intersection point of Sz and the t -axis. Taking $Y = 0$ in equation (2.7) and solving for t we have

$$t_0 = -\frac{[(b_1 - 1)z^2 + 1]}{z[(b_1 + 1)z^4 + (b_1 + 4)z^2 + 3]}.$$
 (4.3)

We see that $|t_0|$ increases as $z \rightarrow 0$.

The straight line $S'z$ obtained from (2.8) also goes through $(t_0, 0)$ and its slope is the slope of Sz with reversed sign.

Let us draw Sz and $S'z$ for values of z going from $z < z_{crit_2}$ to $z > z_{crit_1}$ in the half-plane $Y > 0$.

See Figure 1. We start with $z < z_{crit_2}$. For a fixed z in this region, Sz , $S'z$ and the t -axis define three regions in the half plane $Y > 0$: $tS'z$ bounded by the t -axis and $S'z$; $S'zSz$ bounded by $S'z$ and Sz and tSz bounded by Sz and the t -axis. As z approaches the critical value, Sz and $S'z$ become vertical, so, the region $SzS'z$ for $z < z_{crit_2}$ disappears. When z crosses the critical value, Sz and $S'z$ just change their relative positions. So, in each side of the vertical line, we have three regions tSz , $SzS'z$ and $tS'z$ in the half plane $Y > 0$. In Figure 1, we show Sz and $S'z$ for three different values of z , one value smaller than z_{crit_2} , $z = z_{crit_2}$ and one bigger than z_{crit_2} , but still smaller than zero. To draw Figure 1, we take $b_1 = 8$, $c = 1$.

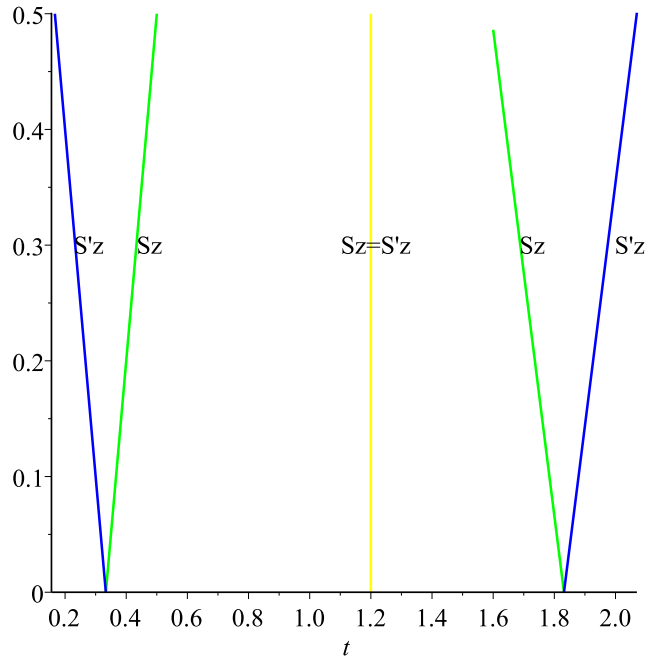


Figure 1: Typical relative positions of Sz (green rays) and $S'z$ (blue rays) for three different values of $z < 0$: $z < z_{crit_2}$, $z = z_{crit_2}$, $z_{crit_2} < z < 0$, yellow ray represents $Sz = S'z$. Here $b_1 = 8$, $c = 1$

Letting z vary, in the half space ($z < 0, t, Y > 0$) there are four regions: one bounded by Son and Son' contained in $z < z_{crit_2}$; one bounded by Son and Son' but contained in $z_{crit_2} < z < 0$. The 3-dimensional regions generated by tSz and $tS'z$ in $z < z_{crit_2}$ connect with its corresponding region in $z_{crit_2} < z < 0$ generating two regions bounded by Son , Son' and \mathcal{C} contained in the half space ($z < 0, t, Y > 0$). Symmetrically, there are four regions in the half space ($z > 0, t, Y > 0$), see Figure 2 which illustrates how \mathcal{C} (plane), Son (green surface) and Son' (blue surface) decompose the wave manifold \mathcal{W} . To draw Figure 2, we take $b_1 = 8$ and $c = 1$.

Let us describe how the three regions in $z_{crit_2} < z < 0$ connect with the three ones in $0 < z < z_{crit_1}$. As $z \rightarrow 0^+$, the intersection point of Sz and $S'z$ goes to $-\infty$, Sz and $S'z$ become the lines $Y = 2c$ and $Y = -2c$, respectively. So, the region under $S'z$ is pushed to $-\infty$ and does not connect to the region on $z < 0$, generating two regions: one above Sz and one limited by Sz and the t -axis. In this way we have six regions in the half space ($z, t, Y > 0$): two regions for $z_{crit_2} < z < z_{crit_1}$; two for $z < z_{crit_2}$ and two for $z > z_{crit_1}$. Symmetrically there are six more regions in the half-space ($z, t, Y < 0$). \square

We will refer to Figure 2 in the description of the twelve regions in \mathcal{W} . *Sonic* and *sonic'* surfaces intersect along the inflection locus (the hyperbola-like curve in the characteristic surface) and also along two vertical lines transversal to the characteristic. We call SS' the 3-dimensional regions contained in $z^2 > 1/(b_1 + 1)$ and bounded by Son , Son' and IL . There are four such regions, which we can specify by the signs of z and Y . We call *lateral regions*, the regions bounded by Son , \mathcal{C} and Son' contained, respectively, in $z > 0$ and in $z < 0$. There are four such regions, again we can specify them by the signs of z and Y . Let us describe the four regions in $z^2 < 1/(b_1 + 1)$. In subspace $Y > 0$, the sonic surface is connected, we call it *bridge*, and the sonic' surface is not connected. We have two regions: the *over bridge* region bounded by Son and Son' and the *under bridge* region bounded by \mathcal{C} , Son and Son' . In subspace $Y < 0$, the *sonic'* surface is connected, we call it *tunnel*, and the sonic surface is not connected. We have two regions: one bounded by Son , Son' and \mathcal{C} , called *over tunnel* and other bounded by Son and Son' , called *under tunnel*.

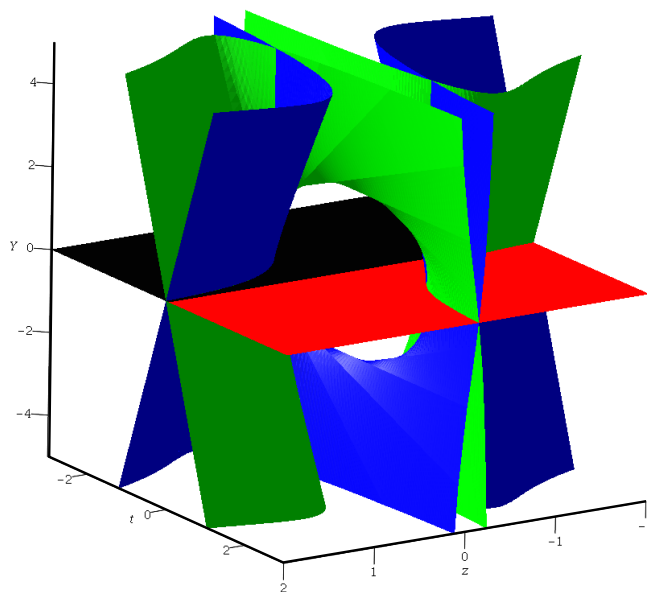


Figure 2: Decomposition of the wave manifold \mathcal{W} in twelve regions defined by \mathcal{C} (plane), Son (green surface) and Son' (blue surface). Here $b_1 = 8$ and $c = 1$

We recall that the coincidence curve on \mathcal{C} is the common boundary of \mathcal{C}_f and \mathcal{C}_s . Hugoniot curves through points of the coincidence curve are tangent to \mathcal{C} and Son' , see [3]. In order to prove this fact in these new coordinates we introduce:

Definition 4. *The two-dimensional sub-manifold of \mathcal{W} generated by Hugoniot curves through points of the coincidence curve is called saturated of the coincidence curve by Hugoniot curves, denoted by SCC .*

Lemma 2. *The surface SCC is tangent to \mathcal{C} and to Son' .*

Proof. A Hugoniot curve through a point of the coincidence curve is given by $2\tilde{U} + b_1 z Y = 2(b_1 u_0 + a_1 - a_4)$, $2(V - c) + Y = 2(v_0 + a_2)$, where (u_0, v_0) is a point of the ellipse

$$\mathcal{E} = (b_1 u_0 + a_1 - a_4)^2 + 4(v_0 + a_3)(v_0 + a_2) = 0. \quad (4.4)$$

Using equations (2.6) in the expressions of u_0 and v_0 and substituting into the ellipse equation 4.4, we get that the surface SCC is given by:

$$\frac{t f_1 Y^2 + t f_2 Y + t f_3}{z^2 + 1} = 0, \quad (4.5)$$

where

$$\begin{aligned} t f_1 &= (z^2 + 1)(b_1^2 z^2 + 4), \\ t f_2 &= 4cz(z^2 + 1)(b_1 z^2 - b_1 + 4)t + 2[(b_1 - 1)z^2 + 1], \\ t f_3 &= 4c^2 t^2 (z^2 + 1)^3. \end{aligned}$$

The intersection of SCC and \mathcal{C} is obtained putting $Y = 0$ in equation (4.5). Doing so, we get $4c^2 t^2 (z^2 + 1)^2 = 0$. It follows that SCC is tangent to \mathcal{C} along the straight line $t = 0$, the coincidence curve.

Hugoniot curves are tangent to Son' along a curve called *hysteresis' curve*, somewhat improperly referred as sonic fold in [3]. To show that SCC surface is tangent to Son' we solve the equation of (2.8) in Y , obtaining

$$Y = \frac{2c[(b_1 + 1)tz^5 + (b_1 + 4)tz^3 + (b_1 - 1)z^2 + 3tz + 1]}{(b_1 + 1)z^4 + b_1 z^2 - 1}. \quad (4.6)$$

By Substituting Y from equation (4.6) into equation (4.5) we obtain

$$4c^2 \left\{ \frac{(1 + z^2)[(b_1 + 1)^2 z^4 + 2(b_1 + 3)z^2 + 1]t + (2 + b_1)z[(b_1 - 1)z^2 + 1]}{(1 + z^2)[(b_1 + 1)z^2 - 1]} \right\}^2 = 0. \quad (4.7)$$

So SCC is tangent to Son' . □

Remark 2. *The surface SCC is topologically a cylinder, each section $z = \text{constant}$ is an ellipse. It is easy to see that all ellipses are tangent to the $t - \text{axis}$ at $(0, 0)$ and contained in the $Y < 0$ half plane. In this way SCC is contained in the $Y < 0$ half space, in fact, in the above tunnel region. The interior of SCC is the saturated of the elliptic region by Hugoniot curves and its exterior is the saturated of the hyperbolic region by Hugoniot curves.*

We emphasize that equation (4.7) is the projection of $Son' \cap SCC$, *hysteresis' curve* on the plane (z, t) .

Parametric equations for *hysteresis' curve* are obtained solving equation (4.7) in t , and substituting $t(z)$ into equation (4.6). Straightforward calculations give the parametric equations as,

$$\begin{cases} z = z, \\ t = -\frac{(b_1 + 2)z[(b_1 - 1)z^2 + 1]}{(z^2 + 1)[(b_1 + 1)^2 z^4 + 2(b_1 + 3)z^2 + 1]}, \\ Y = -\frac{2c[(b_1 - 1)z^2 + 1]}{(b_1 + 1)^2 z^4 + 2(b_1 + 3)z^2 + 1}. \end{cases} \quad (4.8)$$

5 Finding Son'_s and Son'_f

In this section, we describe how Son' splits into *slow sonic' surface*, Son'_s , and *fast sonic' surface*, Son'_f . In order to do so, we will take a point in Son' , the Hugoniot curve through this point, find the intersection with \mathcal{C} , calculate the shock speed in each of these 2 points and see which point of \mathcal{C} has the same speed as our initial point in Son' .

Given a point (t'_0, z_0, Y_0) on Son' , we obtain from equation (2.8) that

$$t'_0 = \frac{Y_0(z_0^2 + 1)[(b_1 + 1)z_0^2 - 1] - 2c[(b_1 - 1)z_0^2 + 1]}{2cz_0(z_0^2 + 1)[(b_1 + 1)z_0^2 + 3]}.$$

The shock speed at this point, $s_{son'}(t'_0, z_0, Y_0)$, is obtained putting $t_0 = t'_0$ into equation (2.9),

$$s_{son'}(t'_0, z_0, Y_0) = \frac{[(b_1 + 1)z_0^2 - 1]^2 Y_0 + 6c(b_1 + 1)z_0^2 + 2c}{2b_1 z_0 [(b_1 + 1)z_0^2 + 3]}. \quad (5.1)$$

Parametric equations for the Hugoniot curve through (t'_0, z_0, Y_0) are obtained changing t_0 into t'_0 in equations (2.12), giving $(t_{hu}(z), z, Y_{hu}(z))$. Solving equation $Y_{hu} = 0$, we obtain the z coordinates of the intersection points of Hugoniot curve with \mathcal{C} ,

$$z_{c_1} = \frac{(b_1 + 1)z_0^2 + 1}{2z_0} \quad \text{and} \quad z_{c_2} = -\frac{2(Y_0 - c)z_0}{(b_1 + 1)Y_0 z_0^2 + Y_0 + 2c}.$$

Substituting z_{c_1} and z_{c_2} in the expression of $t_{hu}(z)$ we obtain, respectively, the t coordinates of the intersection points,

$$t_{c_1} = \frac{2z_0 \left\{ [(b_1 + 1)^2 z_0^4 + 2(b_1 + 3)z_0^2 + 1]Y_0 + 2c[(b_1 - 1)z_0^2 + 1] \right\}}{c[(b_1 + 1)z_0^2 + 3][(b_1 + 1)^2 z_0^4 + 2(b_1 + 3)z_0^2 + 1]}$$

and

$$t_{c_2} = -\frac{(A_{t_{c_2}} Y_0 + B_{t_{c_2}})[(b_1 + 1)z_0^2 + 1]Y_0 + 2c)^2}{2cz_0[(b_1 + 1)z_0^2 + 3](C_{t_{c_2}} Y_0^2 + D_{t_{c_2}} Y_0 + E_{t_{c_2}})},$$

where

$$\begin{aligned}
A_{t_{c_2}} &= (b_1 + 1)^2 z_0^4 + 2(b_1 + 3)z_0^2 + 1, \\
B_{t_{c_2}} &= 2c[(b_1 - 1)z_0^2 + 1], \\
C_{t_{c_2}} &= [(b_1 + 1)^2 z_0^4 + 2(b_1 + 3)z_0^2 + 1], \\
D_{t_{c_2}} &= 4c[(b_1 - 1)z_0^2 + 1], \\
E_{t_{c_2}} &= 4c^2(z_0^2 + 1).
\end{aligned}$$

So, the intersection points of Hugoniot curve with \mathcal{C} are $\mathcal{C}_1 = (t_{c_1}, z_{c_1}, 0)$ and $\mathcal{C}_2 = (t_{c_2}, z_{c_2}, 0)$.

Substituting \mathcal{C}_1 and \mathcal{C}_2 into equation (2.9) we obtain, respectively

$$s_{c_1} = \frac{\left\{ (b_1 + 1)^3 z_0^4 + 2[(b_1 + 1)^2 - 2]z_0^2 + b_1 + 1 \right\} Y_0 + 2c[(b_1 + 1)^2 z_0^2 + 2z_0^2 + b_1 + 1]}{2z_0 b_1 [(b_1 + 1)z_0^2 + 3]}$$

and

$$s_{c_2} = \frac{[(b_1 + 1)z_0^2 - 1]^2 Y_0 + 6c(b_1 + 1)z_0^2 + 2c}{2b_1 z_0 [(b_1 + 1)z_0^2 + 3]}.$$

A simple inspection shows that $s_{c_2} = s_{son'}(t'_0, z_0, Y_0)$.

According to Lemma 1, we must to study the sign of t_{c_2} . If $t_{c_2} > 0$, the point (t'_0, z_0, Y_0) is in Son'_f , otherwise it is in Son'_s .

Proposition 2. *The hysteresis' curve and the straight line $(t, z = 0, Y = -2c)$ are the boundaries of Son'_s and Son'_f .*

Proof. We have to study the sign of t_{c_2} . The denominator is the product of $2cz_0[(b_1 + 1)z_0^2 + 3]$ and a polynomial of degree 2 in Y_0 with negative discriminant. Since the coefficient of Y_0^2 is positive the denominator has the same sign as z_0 . The numerator is a term of the form $A(z_0)Y_0 + B(z_0)$, A and B positives, multiplied by a positive term, everything preceded by a minus sign.

It follows that the curves $z = 0$ and $AY + B = 0$, in Son' , are the boundaries of Son'_s and Son'_f . If $Y > -B/A$ and $z > 0$ the point is in Son'_s , switching according to sign change.

The curve $AY + B = 0$ is the projection of hysteresis' curve on zY plane (the third equation in (4.8)). In Son' , $z = 0$ is the straight line $(t, z = 0, Y = -2c)$. It is the intersection of Son' with the surface SSB , the saturated of the secondary bifurcation by Hugoniot curves, (see Appendix 1). The straight line and the hysteresis' curve intersect transversely forming a saddle point in Son' . \square

6 Lax's Shocks in \mathcal{W}

In this section, we introduce Admissibility condition for Hugoniot arcs in \mathcal{W} . By arc we mean the image of a closed interval. There will be two types of conditions, which are called simply type 1 and type 2.

We begin by introducing two simplifying assumptions, [1]:

Giving a point $\mathcal{U} \in \mathcal{W}$, we use $sh(\mathcal{U})$ ($sh'(\mathcal{U})$) to denote the Hugoniot (Hugoniot') curve through \mathcal{U} . We define \mathcal{U}_s , \mathcal{U}_f , \mathcal{U}'_s and \mathcal{U}'_f to be the points

$$\mathcal{U}_s = sh(\mathcal{U}) \cap \mathcal{C}_s, \quad \mathcal{U}_f = sh(\mathcal{U}) \cap \mathcal{C}_f, \quad \mathcal{U}'_s = sh'(\mathcal{U}) \cap \mathcal{C}_s, \quad \text{and} \quad \mathcal{U}'_f = sh'(\mathcal{U}) \cap \mathcal{C}_f. \quad (6.1)$$

These points are fundamental to obtain the characteristic speed, λ_s (or λ_f), associated to \mathcal{U} , see Fig. 3.

Assumption 6.1. *We will deal only with points \mathcal{U} on \mathcal{W} such that the points \mathcal{U}_s and \mathcal{U}_f always exist, i.e., in the hyperbolic region.*

Assumption 6.2. *We consider only Hugoniot and Hugoniot' curves that are diffeomorphic to \mathbb{R} , i.e., they do not contain points in the secondary bifurcation locus.*

Let us consider a fixed $\mathcal{U} \in \mathcal{W}$ and we use (6.1) to define $\mathcal{U}'_s, \mathcal{U}'_f$,

1.- The Lax's shock of type 1:

$$s(\tilde{\mathcal{U}}) < s(\mathcal{U}_s) = \lambda_s(\mathcal{U}) \quad \lambda_s(\mathcal{U}') = s(\tilde{\mathcal{U}}'_s) < s(\tilde{\mathcal{U}}) < \lambda_f(\mathcal{U}'). \quad (6.2)$$

2.- The Lax's shock of type 2:

$$s(\tilde{\mathcal{U}}) > s(\mathcal{U}_f) = \lambda_f(\mathcal{U}) \quad \lambda_s(\mathcal{U}') = s(\mathcal{U}'_s) < s(\tilde{\mathcal{U}}) < s(\mathcal{U}'_f) = \lambda_f(\mathcal{U}'). \quad (6.3)$$

Following the physics, Lax defines one- and two- shocks. Any of these shocks is a pair of states that satisfies the Rankine-Hugoniot equation and certain speed inequalities. Therefore, the definition *shock*, *1-shock*, *2-shock* applies to points in the wave manifold, not to curves in the wave manifold. For the purpose of the topological construction of Riemann solutions, which is the object of this paper, it is may be convenient to use this nomenclature for certain curves of shock points in the wave manifold consisting of either 1-shocks or 2-shocks. It is also convenient to provide an orientation to these curves. So we use the nomenclature *forward shock curve* to a curve oriented with decreasing speed consisting of 1-shocks. Similarly, *backward shock curve* to a curve oriented with increasing speed consisting of 2-shocks. Other combination of orientations or Lax type are not necessary in this paper and will not be used. However, if any of these shocks are needed, they will receive their full name, for instance, *1-backward shock*; or *2-forward shock*.

A Hugoniot arc curve is a *forward shock curve* if is oriented with decreasing speed and satisfies the following conditions, [1] :

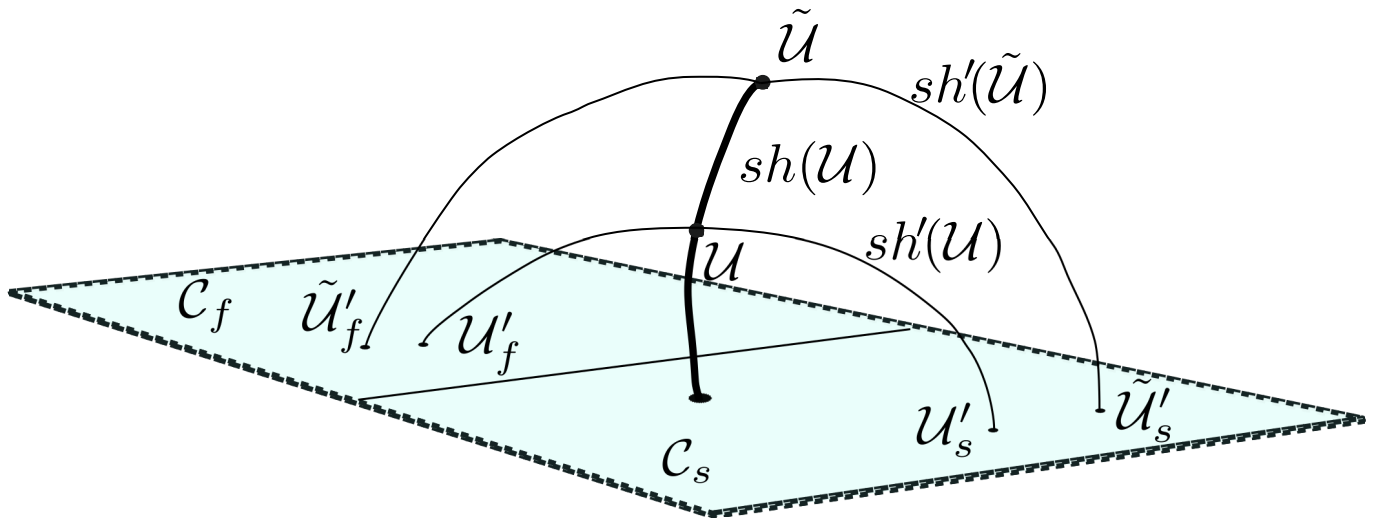


Figure 3: Consider $\mathcal{U} \in \mathcal{W}$. From \mathcal{U} , we take a $\tilde{\mathcal{U}} \in sh(\mathcal{U})$. We obtain the projections of \mathcal{U} and $\tilde{\mathcal{U}}$ in \mathcal{C}_s and \mathcal{C}_f using Hugoniot' curves, denoted as $\mathcal{U}'_s, \tilde{\mathcal{U}}'_s, \mathcal{U}'_f$ and $\tilde{\mathcal{U}}'_f$.

L1.1- The speed s at any point \mathcal{U} in the arc satisfies $s(\mathcal{U}) \leq s(\mathcal{U}_s)$,

L1.2- The speed s at any point \mathcal{U} in the arc satisfies $s(\mathcal{U}'_s) \leq s(\mathcal{U}) \leq s(\mathcal{U}'_f)$.

It follows that:

- 1.- Since a forward shock curve is oriented with decreasing speed, it stops if it reaches Son , otherwise it goes to infinity (as s decreases and z goes to plus or minus infinity)
- 2.- From condition **L1.1** a forward shock curve begins at C_s or Son'_s .

Forward shock curves starting at C_s are called *local* and forward shock curves starting at Son'_s are called *nonlocal*.

By continuity of s , given a Hugoniot arc with decreasing s , starting at C_s or in Son'_s and ending in Son or at infinity, it is sufficient to check conditions **L1.1** or **L1.2** at the initial point, to verify whether it is a forward shock curve or not.

Since both conditions are trivially satisfied in C_s and **L1.1** is also trivially in Son'_s , it is sufficient to verify **L1.2** at Son'_s for the arc to be a forward shock curve.

In the same way, a Hugoniot arc curve is said a (a backward shock curve) if is oriented with increasing speed and satisfies the following conditions, [1]:

L2.1- The speed s at any point \mathcal{U} in the arc satisfies $s(\mathcal{U}) \geq s(\mathcal{U}_f)$;

L2.2- The speed s at any point \mathcal{U} in the arc satisfies $s(\mathcal{U}'_s) \leq s(\mathcal{U}) \leq s(\mathcal{U}'_f)$.

It follows that:

- 1.- Since a backward shock curve is oriented with increasing speed, it stops if it reaches Son , otherwise it goes to infinity (as s increases and z goes to plus or minus infinity.)
- 2.- From condition **L2.1** a backward shock curve begins at C_f or Son'_f . Backward shock curves starting at C_f are called *local* and backward shock curves starting at Son'_f are called *nonlocal*.

By continuity of s , giving a Hugoniot arc with increasing s , starting at C_f or in Son'_f and ending in Son or at infinity, it is sufficient to check conditions **L2.1** and **L2.2** at the initial point to verify whether it is a backward sock curve or not. Since both conditions are trivially satisfied in C_f , and **L2.1** is also trivially satisfied in Son'_s , it is sufficient to verify **L2.2** at Son'_s for the arc to be a backward shock curve.

Remark 3. Since conditions **L1.2** and **L2.2** are the same, we refer to them simply as **L2**.

7 Rarefactions and Composites

7.1 Rarefactions

Going back to equation $W_t + F(W)_x = 0$, we will consider solutions of the form $\widetilde{W}(x/t)$, which will be called *rarefaction waves*. So, our equation becomes

$$(-x/t^2)\widetilde{W}' + (1/t)DF(\widetilde{W})\cdot\widetilde{W}' = 0,$$

where $\widetilde{W} = \widetilde{W}(\lambda)$, $\lambda = x/t$ and ' indicates differentiation with respect to λ .

We see that the curves parametrically defined in the (u, v) -plane by the rarefaction waves are the integral curves of the line fields defined by the eigenvectors of $DF(u, v)$. We call these curves *rarefaction curves*.

For F given by (2.1) we have

$$DF = \begin{bmatrix} (b_1 + 1)u + a_1 & v + a_2 \\ v + a_3 & u + a_4 \end{bmatrix}$$

Let $r = (r_1, r_2)$ be the eigenvector associated to the eigenvalue λ . Eliminating λ in the system

$$\begin{cases} [(b_1 + 1)u + a_1]r_1 + (v + a_2)r_2 = \lambda r_1 \\ (a_3 + v)r_1 + (a_4 + u)r_2 = \lambda r_2. \end{cases}$$

and replacing r_1/r_2 by du/dv we get the differential equation:

$$(v + a_3) \left(\frac{du}{dv} \right)^2 - (b_1 u + a_1 - a_4) \frac{du}{dv} - (v + a_2) = 0.$$

Let Δ be the discriminant of this 2nd degree equation in du/dv ,

$$\Delta = (b_1 u + a_1 - a_4)^2 + 4(v + a_2)(v + a_3).$$

When $\Delta = 0$, the equation of the *coincidence curve* defined in Subsection 2.1, it is an ellipse. As stated before, its interior is called elliptic region, and there are no rarefaction curves there. The exterior of ellipse is called hyperbolic region and here, through every point pass two rarefaction curves transversal to each other.

To study this differential equation, we introduce a new variable z , and replace the differential equation by the pair of equations

$$\begin{cases} G_2 = (v + a_3)z^2 - (b_1 u + a_1 - a_4)z - (v + a_2) = 0 \\ z dv - du = 0. \end{cases}$$

which we see as a differential equation in a surface in (u, v, z) -space. Since z is a direction, (u, v, z) -space is actually $\mathbb{R}^2 \times \mathbb{R}P^1$.

The integral curves of $z dv - du = 0$ in this surface are also called *rarefaction curves*. Their projections onto the (u, v) -plane by $(u, v, z) \rightarrow (u, v)$ are the rarefaction curves defined above.

By introducing new variables: $\widetilde{U} = b_1 u + a_1 - a_4$ and $V_1 = v + a_2$, the expression of G_2 becomes G , *i.e.*, the equation of surface is written as $G = 0$, so, if we consider (\widetilde{U}, V_1, z) -space as naturally embedded in $(\widetilde{U}, V_1, X, Y, z)$ -space defined in Section 2, we see that the surface introduced here is precisely the characteristic surface defined there, by $G = 0, Y = 0$.

Let us use the second equation of the system

$$\begin{cases} [(b_1 + 1)u + a_1]r_1 + (v + a_2)r_2 = \lambda r_1, \\ (a_3 + v)r_1 + (a_4 + u)r_2 = \lambda r_2 \end{cases}$$

to define λ as a function of u, v and z , using that $z = r_1/r_2$. If we replace u and v by the new coordinates \widetilde{U}, V_1 , we see that λ coincides with s defined in Section 2 as a function of $(\widetilde{U}, V_1, Y, z)$, when $z = 0$, and the inflection locus defined there as the intersection of Son with \mathcal{C} can also be defined as the

set of points where λ is critical along the rarefaction curves.

The curve defined in the characteristic surface by $G = 0$ and $\partial G/\partial z = 0$ is where the tangent plane to the characteristic surface is vertical, and projects onto the coincidence curve, so, it is also called *coincidence curve*. It separates \mathcal{C} into two components, which are \mathcal{C}_s and \mathcal{C}_f defined before.

A complete study of rarefactions can be found in [8] and in [2] and a formal definition of rarefactions in the wave manifold can be found in [5] and in [2].

Let us obtain the differential equation of the rarefaction curves in t and z coordinates. Replacing u and v by \tilde{U} and V_1 , the equation $zdv - du = 0$ becomes $b_1 z dV_1 - d\tilde{U} = 0$. Take the expressions of \tilde{U} and V_1 in terms of t and z , $\tilde{U} = 2cz/(z^2 + 1) + ct(z^2 - 1)$, $V_1 = c/(z^2 + 1) + ctz$ differentiate, and replace $d\tilde{U}$ and dV_1 by their expressions in dt and dz . Collecting terms, we arrive at

$$\frac{dt}{dz} = \frac{-t(b_1 - 2)z^5 - 2t(b_1 - 2)z^3 + 2(b_1 - 1)z^2 - t(b_1 - 2)z + 2}{(z^2 + 1)^2(1 + (b_1 - 1)z^2)}. \quad (7.1)$$

In this context it is important to orient the rarefaction curves according to the growth of s (or, which is the same λ).

For the purpose of this paper we, will define a *forward rarefaction* to be a rarefaction arc in \mathcal{C}_s with increasing s . We will define a *backward rarefaction* to be a rarefaction arc in \mathcal{C}_f with decreasing s .

The expression of s in terms of z and t (as we have seen in Section 2, s does not depend on Y) is given by equation (2.9). The variation of s along a rarefaction curve is given by $ds/dz = \partial s/\partial z + (\partial s/\partial t)(dt/dz)$, where dt/dz is the differential equation (7.1).

After simplification, we arrive at

$$\frac{ds}{dz} = \frac{z(z^2 + 1)[(b_1 + 1)z^2 + 3]t + (b_1 - 1)z^2 + 1}{[(b_1 - 1)z^2 + 1](z^2 + 1)}.$$

Since the denominator is positive, we only need to look at the numerator, which is of the form $A(z)t + B(z)$. The equation $A(z)t + B(z) = 0$ defines the curve where s is critical along the rarefaction curves. This is exactly the inflection locus, defined in Section 2 as the intersection of the sonic surface Son with the characteristic surface \mathcal{C} . Just put $Y = 0$ in the equation of Son .

In z, t coordinates, the inflection locus looks like the hyperbola $t = -1/z$. The derivative ds/dz is clearly positive between the two branches and negative in the two other regions (“exterior” to the two branches), so, a rarefaction curve will be oriented in the direction of increasing z between the branches and in the direction of decreasing z out of the branches. As shown in figure ???? a rarefaction curve arrives at the inflection locus, in \mathcal{C}_s ($t < 0$) and leaves the inflection locus in \mathcal{C}_f ($t > 0$) and this remains true even if the rarefaction curve is tangent to the inflection locus. As a consequence, at such a tangency point, the rarefaction curve necessarily crosses the inflection locus. As will be seen in Section 8, there are two such points. We denote by \mathcal{I}_s and \mathcal{I}_f the branches of the inflection locus in \mathcal{C}_s and \mathcal{C}_f .

7.2 Composites

Given a point \mathcal{U} in Son' , the Hugoniot curve through \mathcal{U} generically intersects \mathcal{C} in two points, \mathcal{U}_s and \mathcal{U}_f such that either $s(\mathcal{U}_s) = s(\mathcal{U})$ or $s(\mathcal{U}_f) = s(\mathcal{U})$. This allows us to define a projection T from Son' to \mathcal{C} which takes \mathcal{U} into \mathcal{U}_s or \mathcal{U}_f such that $s(T(\mathcal{U})) = s(\mathcal{U})$. The pullback of rarefaction curves from \mathcal{C} to Son' are called *composite curves*. They are described in [3].

We can obtain the differential equation of the composite curves in coordinates z and Y . As seen in Section 5, given a point $(z_1, Y_1, t(z_1, Y_1))$ in Son' the map which associates the point in \mathcal{C} in the same Hugoniot curve through $(z_1, Y_1, t(z_1, Y_1))$ and with the same value of the speed $s(z_1, Y_1, t(z_1, Y_1))$, is given by $(z_1, Y_1) \rightarrow (z_{c_2}, t_{c_2})$, where

$$z_{c_2} = -\frac{2(Y_1 - c)z_1}{2b_1 z_1 [(b_1 + 1)z_1^2 + 3]} \quad \text{and} \quad t_{c_2} = \frac{(A_{t_{c_2}} Y_1 + B_{t_{c_2}}) [(b_1 + 1)z_1^2 + 1] Y_1 + 2c)^2}{2c z_1 [(b_1 + 1)z_1^2 + 3] (C_{t_{c_2}} Y_1^2 + D_{t_{c_2}} Y_1 + E_{t_{c_2}})},$$

where

$$\begin{aligned} A_{t_{c_2}} &= (b_1 + 1)z_1^4 + 2(b_1 + 3)z_1^2 + 1, \\ B_{t_{c_2}} &= -2c[(b_1 - 1)z_1^2 + 1], \\ C_{t_{c_2}} &= Y_1^2 [b_1 + 1z_1^4 + 2(b_1 + 3)z_1^2 + 1], \\ D_{t_{c_2}} &= 4cY_1 [(b_1 - 1)z_1^2 + 1], \\ E_{t_{c_2}} &= 4cY_1 [(b_1 - 1)z_1^2 + 1] + 4c^2 (z_1^2 + 1). \end{aligned}$$

To avoid confusion, we use z_1 and Y_1 as coordinates in Son' . To get the composite differential equation, we write equation (7.1) in the form $m(z, t)dz + n(z, t)dt = 0$. Replacing $m(z, t)$ by $m(z_{c_2}(z_1, Y_1), t_{c_2}(z_1, Y_1))$, $n(z, t)$ by $n(z_{c_2}(z_1, Y_1), t_{c_2}(z_1, Y_1))$, dz by $(\partial z_{c_2} / \partial z_1) dz_1 + (\partial z_{c_2} / \partial Y_1) dY_1$ and dt by $(\partial t_{c_2} / \partial z_1) dz_1 + (\partial t_{c_2} / \partial Y_1) dY_1$, after simplification, we get the composite differential equation given by

$$\frac{[(\mu_2(z_1)Y_1^2 + \mu_1(z_1)Y_1 + \mu_0(z_1))]}{z_1((b_1 + 1)z_1^2 + 3)} dz_1 + [\nu_1(z_1)Y_1 + \nu_0(z_1)] dY_1, \quad (7.2)$$

where

$$\begin{aligned} \mu_2(z_1) &= -(b_1 + 1)^4 z_1^8 - 4(2b_1 + 3)(b_1 + 1)^2 z_1^6 - 2(b_1 + 1)(13b_1 + 1)z_1^4 + 12z_1^2 + 3, \\ \mu_1(z_1) &= 4c[(b_1 + 1)^2 z_1^6 + (b_1 + 1)(5b_1 - 7)z_1^4 + 3(z_1^2 + 1)], \\ \mu_0(z_1) &= -12c^2 [(b_1 + 1)z_1^2 - 1][(b_1 - 1)z_1^2 + 1], \\ \nu_1(z_1) &= -[(b_1 + 1)^3 z_1^6 + (b_1 + 1)(7b_1 - 1)z_1^4 + (7b_1 - 1)z_1^2 + 1], \\ \nu_0(z_1) &= 2c[(b_1 + 1)z_1^2 - 1][(b_1 - 1)z_1^2 + 1]. \end{aligned}$$

The equation (7.2) is singular at points $(z_2 = -1/\sqrt{b_1 + 1}, Y_1 = 0)$ and $(z_1 = 1/\sqrt{b_1 + 1}, Y_1 = 0)$, such points are, respectively, the intersection points of the double sonic locus $(z = z_{crit_2}, t = t_2, Y)$ and $(z = z_{crit_1}, t = t_1, Y)$ with the Characteristic surface. The differential equation is not defined at $z_1 = 0$. In fact, besides these two singularities there are two other ones at $z_1 = 0$ and $z_1 = \infty$, both of type saddle, see [3].

In the same way as for rarefaction curves, it is important to orient the composite curves according to the growth of s .

For the purpose of this paper, we will define *local forward composite* to be a composite arc in Son'_s starting at \mathcal{I}_s with decreasing s . We will define *local backward composite* to be a composite arc in Son'_f starting at \mathcal{I}_f with increasing s .

8 Wave Curves

In this section, we construct wave curves in the wave manifold \mathcal{W} . A wave curve in \mathcal{W} is a succession of rarefaction, shock and composite waves (forward and backward) satisfying certain conditions. Our list is not complete, not all possibilities are described, we focus only wave curves used here. We follow Section 4 of [1].

8.1 Local Wave Curves

We begin by constructing a local forward wave curve as follows: start with a point P_0 in \mathcal{C}_s . Let s_0 be the value of the speed at P_0 . The first arc is a forward rarefaction, contained in \mathcal{C}_s , starting at P_0 , with speed increasing s . It is easy to see that there are only two possibilities: either the arc stops at the inflection locus (s stops increasing) or the arc stops at the coincidence locus (the arc leaves \mathcal{C}_s). Let P_1 be the end point at this forward rarefaction arc. The second arc is a forward shock arc starting at P_0 , with decreasing speed s . Again there are two possibilities. Either the arc goes to infinity, or it stops at a point P_2 in the sonic surface (s stops decreasing).

If P_1 is on the coincidence locus, the wave curve stops there. If there is no point P_2 , the wave curve is an infinite forward shock arc starting at P_0 , or $Sh_{P_0\infty}$, and the forward rarefaction from P_0 to P_1 , RP_0P_1 .

If P_1 is on the inflection locus, we add a third arc: the forward composite arc starting at P_1 with decreasing s , which will stop at a point P_3 on Son' , with speed s_3 , namely $Co_{P_1P_3}$. The latter is either at the double contact (double sonic locus), or $s_3 = s_1$, whichever comes first.

In case $s_3 = s_1$, we add the non-local forward shock arc starting at P_3 with decreasing s until P_6 , $NLSh_{P_3P_6}$. If P_3 is on the double contact, we consider the auxiliary Hugoniot' arc starting at P_3 , $hug'_{P_3P_4}$. The arc will hit \mathcal{C}_s at a point P_4 . From P_4 we take the forward rarefaction until P_5 , contained in \mathcal{C}_s , RP_4P_5 with increasing s .

We may summarize as:

- **Case 1-** For P_1 on the coincidence locus. The wave curve is $Sh_{P_0\infty} \cup RP_0P_1$. The speed s decreases along shock arc and increases along rarefaction arc.
- **Case 2-** For P_1 on the inflection locus and $s_3 = s_1$. The wave curve is $Sh_{P_0\infty} \cup RP_0P_1 \cup Co_{P_1P_3} \cup NLSh_{P_3P_6}$. The speed s decreases along shock and composite arcs and increases along the rarefaction arc.
- **Case 3-** For P_3 on the double contact. The wave curve is $Sh_{P_0\infty} \cup RP_0P_1 \cup Co_{P_1P_3} \cup hug'_{P_3P_4} \cup RP_4P_5$. The speed s decreases along the shock and composite arcs and increases along the rarefaction arcs.

We have 3 more cases, replacing infinity by a point P_2 on Son .

We define a local backward wave curves from a point $P_0 \in \mathcal{C}_f$ as a succession of a backward rarefaction, a local backward shock and a local backward composite. We can also describe similar wave curves for backward arcs.

We remark that wave curves in the wave manifold are not smooth objects, in case 3 they are not even continuous. The intermediate surfaces, introduced in [1], are the better correspondent in the wave manifold for the wave curves in the state space.

8.2 Decomposing C_s according to wave curves structures

To obtain local forward wave curves we need to divide C_s into regions such that wave curves starting at points of each region have similar properties.

We know that along rarefaction curves in C_s the speed s increases towards \mathcal{I}_s , *i.e.*, for a given state in $(z, t) \in C_s$:

- 1.- If (z, t) lies on the left side of \mathcal{I}_s , then the forward rarefaction through it, is constructed with increasing values of z .
- 2.- If (z, t) lies on the right side of \mathcal{I}_s , then the forward rarefaction through it, is constructed with decreasing values of z .

In our model, there are states (z, t) for which the forward rarefaction through these points reaches \mathcal{I}_s , as well as there are states for which the forward rarefaction through it, does not reach \mathcal{I}_s . In the second case, the forward rarefaction stops at the coincidence curve, the boundary of C_s and C_f . So, it is necessary to decompose C_s in regions for which these different behaviors occur.

To obtain this decomposition, we look for points (z, t) for which a rarefaction curve and the inflection curve \mathcal{I} are tangent. Differentiating the equation of the inflection curve (4.1) with respect to z , we get:

$$\frac{dt}{dz} = \frac{3z^2 b_1 + b_1 + 4}{(z^2 + 1)^2 (3 + (b_1 + 1)z^2)}. \quad (8.1)$$

Now, equating (8.1) to the rarefaction field given by (7.1), with t given by (4.1), we get that the z coordinates of the tangency points are the roots of:

$$\frac{-3 + (3b_1 + 3)z^2}{(3 + (b_1 + 1)z^2)^2 z^2} = 0, \quad (8.2)$$

$z_1 = 1/\sqrt{b_1 + 1}$ and $z_2 = -1/\sqrt{b_1 + 1}$, *i.e.*, the rarefaction curve and the inflection curve, \mathcal{I} , are tangent at the intersection points of \mathcal{C} with the double contact, (z_{crit_1}, t_1, Y) and (z_{crit_2}, t_2, Y) .

We have proved the following:

Proposition 3. *The rarefaction and inflection curves are tangent at the states $(z_{crit_1}, t_1) \in C_s$ and $(z_{crit_2}, t_2) \in C_f$.*

Rarefaction curves through (z_{crit_1}, t_1) and (z_{crit_2}, t_2) subdivide C_s into three regions:

The rarefaction curve through (z_{crit_2}, t_2) with $z \leq z_{crit_2}$ is denoted by \mathcal{R}_f . This curve reaches $t = 0$ at a point \hat{z} . Let L_1 and L_2 be the straight lines $(z, 0)$ with $z \leq \hat{z}$ and $z > \hat{z}$, respectively. The part of \mathcal{R}_f for $z \leq \hat{z}$ is denoted as \mathcal{R}_{fs} . The region I_a is formed by states (z, t) between L_1 and \mathcal{R}_{fs} . The region I_b is formed by states (z, t) between $\mathcal{R}_{fs} \cup L_2$ and $\mathcal{R}_s \cup \mathcal{I}_s$ ($z > z_{crit_1}$). We define the region I as $I_a \cup I_b$. The region II is formed by states (z, t) below \mathcal{R}_s and on the left side of \mathcal{I}_s ($z < z_{crit_1}$). The region III is formed by states (z, t) on the right side of \mathcal{I}_s , see Fig. 4.

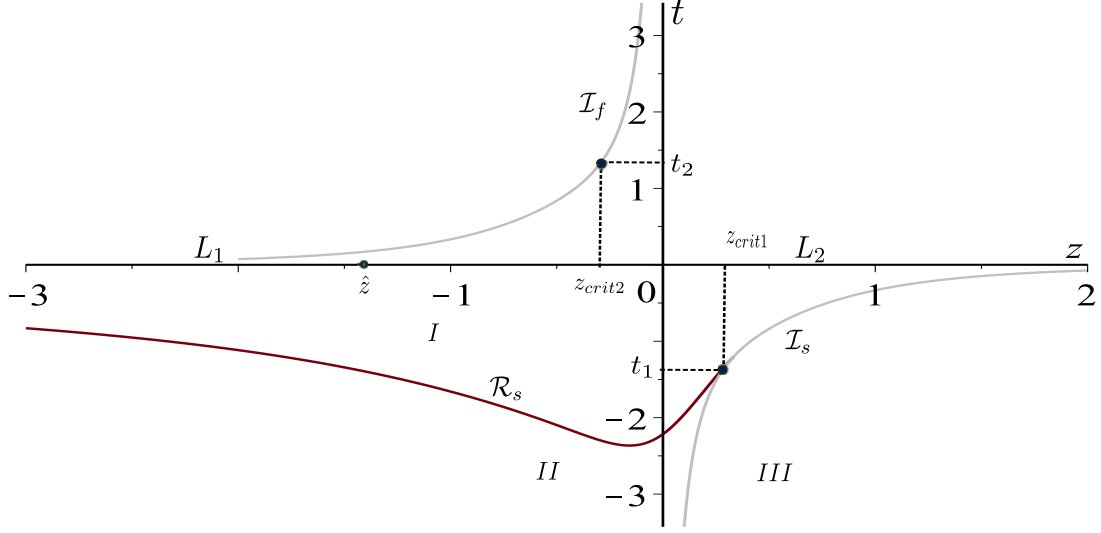


Figure 4: The three regions defined in \mathcal{C}_s . The branch of inflection in \mathcal{C}_s is denoted by \mathcal{I}_s and the branch of inflection in \mathcal{C}_f is denoted by \mathcal{I}_f .

9 Riemann Solution

The Riemann solution is constructed by using the wave curves defined in the Section 8. For a pair (W_L, W_R) given in the hyperbolic region, we utilize the following algorithm to obtain the solution.

Algorithm RS:

- For a pair (W_L, W_R) both given in hyperbolic region in the phase space, by substituting $W_L = (u_L, v_L)$ into (2.10) and setting $Y = 0$, we obtain two states in the wave manifold \mathcal{W} : $\mathcal{U}_L = (z_1, t_1 < 0, 0)_L \in \mathcal{C}_s$ and $\tilde{\mathcal{U}}_L = (z_2, t_2 > 0, 0)_L \in \mathcal{C}_f$.
- Similarly, by substituting $W_R = (u_R, v_R)$ into (2.10) and setting $Y = 0$, we obtain two states in the wave manifold \mathcal{W} : $\tilde{\mathcal{U}}_R = (z_1, t_1 < 0, 0)_R \in \mathcal{C}_s$ and $\mathcal{U}_R = (z_2, t_2 > 0, 0)_R \in \mathcal{C}_f$.
- To construct the solution, we utilize the states \mathcal{U}_L and \mathcal{U}_R .
- From \mathcal{U}_L we draw the waves of 1-family, described in Subsection 8.
- After we constructed the 1-family, we saturated the curves as described in Subsection 9.3.
- From the state \mathcal{U}_R , we construct the wave of 2-reverse wave sequence, described in Section 9.4.
- The Riemann solution consists of in the sequence of waves and states obtained through the intersection between the saturated surface through \mathcal{U}_L and the 2-reverse wave through \mathcal{U}_L .
- After, we obtain the solution on the plane w .

Remark 4. The Riemann solution is a sequence of shocks, rarefactions and constant states. In the wave manifold \mathcal{W} , we denote:

- Hugoniot curve arcs: \mathcal{H}_1 for curves starting at $t < 0$ and \mathcal{H}_2 starting at $t > 0$.

- Rarefaction curves: \mathcal{R}_1 for curves starting at $t < 0$ and \mathcal{H}_2 starting at $t > 0$.
- Composite curves: \mathcal{C}_1 for curves starting at $t < 0$ and \mathcal{C}_2 starting at $t > 0$.

Given a state $U \in \mathcal{W}$, if the wave through this state z is positive, then identify this wave on right of U . On the other hand, if z is negative the wave is identified on left of U . For instance, from state U we have a \mathcal{R}_1 followed by \mathcal{C}_1 for increasing z and \mathcal{H}_1 for decreasing z , we denote this sequence through U as $\mathcal{H}_1 U \mathcal{R}_1 \mathcal{C}_1$. The saturated surfaces follow the same sequence of waves.

Remark 5. It is necessary to verify that the wave sequence satisfies the geometrical compatibility, i.e., the waves in the sequence have increasing speed.

In the following sections, we divide the \mathcal{C}_s into different parts for which the solution is equal in each region. With these structures, we can obtain the Riemann solution.

9.1 The wave curves in each region

In this section, we describe the construction of local forward wave curves in each of the four regions I to III , in $\mathcal{M} - \Pi$, the interpretation of such wave curve in the (u, v) -plane will be seen in Subsection 9.2.

We consider a state $(z_i, t_i) \in I$, we refer to Fig. 5.

- *Rarefaction*: In this case a rarefaction curve does not cross the inflection \mathcal{I} (neither \mathcal{I}_s nor \mathcal{I}_f). We construct the forward rarefaction \mathcal{R}_1 starting at (z_i, t_i) . \mathcal{R}_1 to L_1 at $(\tilde{z}, 0)$. We stop the construction of rarefaction because from this point we will have a rarefaction in \mathcal{C}_f .
- *Hugoniot*: From (z_i, t_i) we construct the local forward shock arc \mathcal{H}_1 , with decreasing s (decreasing values of z).

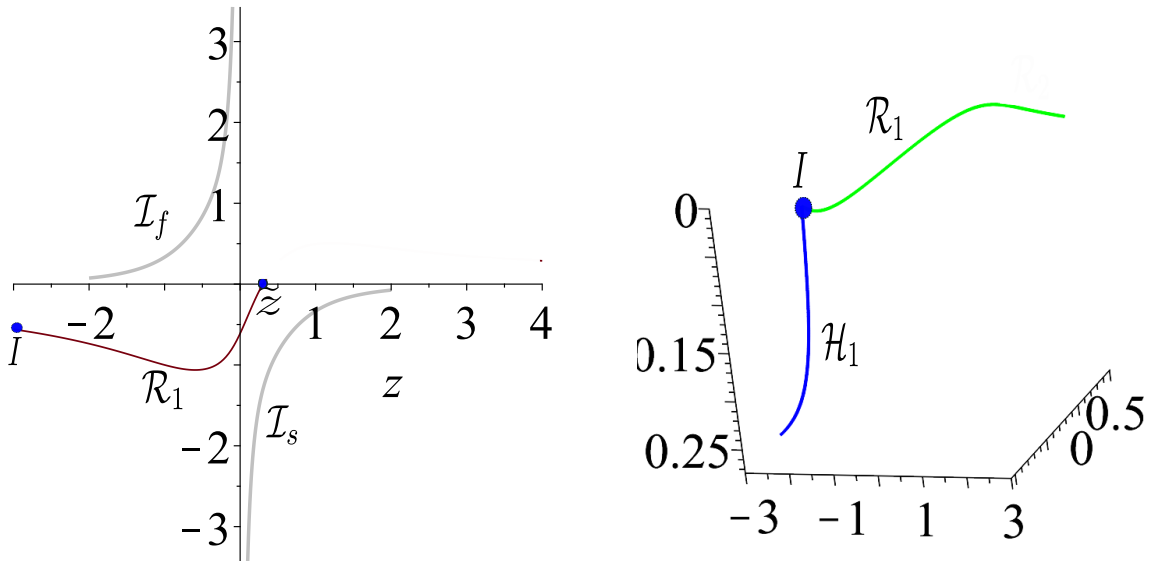


Figure 5: Waves sequence for initial data in region II . Left a:- The rarefaction \mathcal{R}_1 in the characteristic plane \mathcal{C} . Right b:- The wave sequence $\mathcal{H}_1, \mathcal{R}_1$, in $\mathcal{W} - \Pi$.

For a state $(z_i, t_i) \in II$, we refer to Fig. 6.

- *Rarefaction*: From (z_i, t_i) we construct the forward rarefaction \mathcal{R}_1 . This rarefaction intersects the branch \mathcal{I}_s of the inflection curve at (z^\dagger, t^\dagger) , $z^\dagger < z_{crit_1}$.
- *Composite*: From (z^\dagger, t^\dagger) we construct the forward composite \mathcal{C}_1 parameterized by z , $z^\dagger \leq z \leq z_{crit_1}$.
- *Hugoniot*: The forward shock curve arc \mathcal{H}_1 is constructed for decreasing s (decreasing values of z).

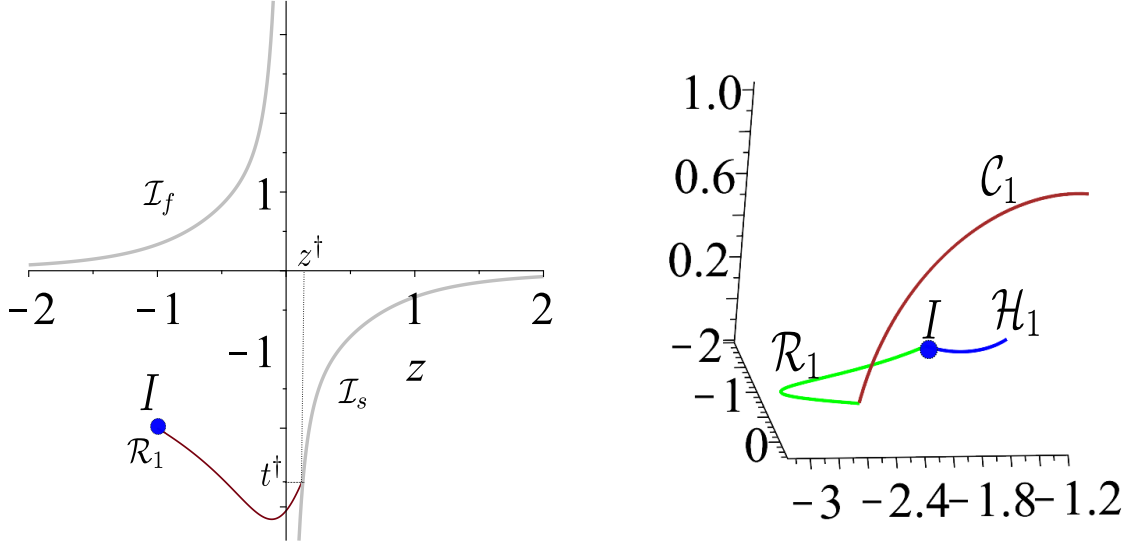


Figure 6: Waves sequence for initial data in region II . *Left a:)-* The rarefactions \mathcal{R}_1 in \mathcal{C} reaches the branch of inflection \mathcal{I}_s . *Right b:)-* The wave sequence \mathcal{H}_1 , \mathcal{R}_1 and \mathcal{C}_1 in $\mathcal{W} - \Pi$.

For a state $(z_i, t_i) \in III$, we refer to Fig. 7.

- *Rarefaction*: From (z_i, t_i) , we construct the forward rarefaction \mathcal{R}_1 up to (z^\dagger, t^\dagger) , the intersection $\mathcal{R}_1 \cap \mathcal{I}_s$, $z_{crit_2} < z^\dagger < z_{crit_1}$.
- *Composite*: From (z^\dagger, t^\dagger) we construct the forward composite \mathcal{C}_1 parameterized by z , $z^\dagger \leq z \leq z_{crit_1}$.
- *Hugoniot*: From (z_i, t_i) we construct the forward shock curve arc \mathcal{H}_1 for decreasing s (increasing values of z).

9.2 The wave curves on the plane uv

The construction of the local forward wave curve in $\mathcal{W} - \Pi$ allow us to obtain the sequence of the 1-waves curves in the original state space, the uv -plane.

Remark 6. *The meaning of colors used in this paper by software TORS to represent rarefactions, shocks, composites etc... do not have the same meaning of the colors used by the software ELI.*

From the wave sequence defined in Subsection 9.1, we utilize the mapping between the wave manifold $\mathcal{W} - \Pi$ and the plane uv given by the equations (9.11) – (9.13).

There is a mapping between the elliptic boundary and the SCC . An interesting feature is that the straight line $(z, t = 0)$ in the \mathcal{W} represents the elliptic boundary on the plane uv .

Here, we obtain the same sequence of waves in each region I to III (of wave manifold \mathcal{W} in \mathcal{C}_s) on the plane uv .

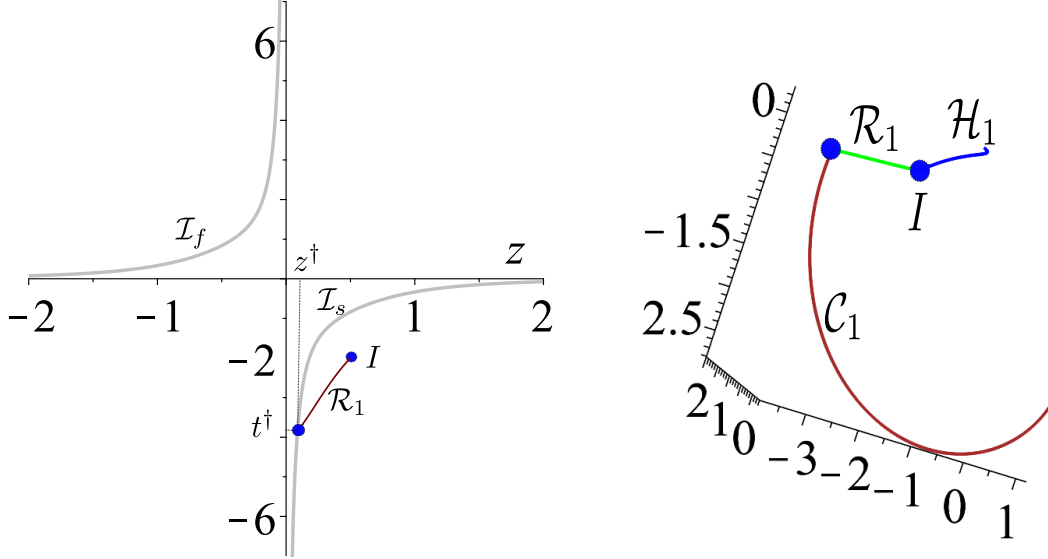


Figure 7: Waves sequence for initial data in region III . *Left a:-* The rarefactions \mathcal{R}_1 in \mathcal{C} reaches the branch of inflection \mathcal{I}_s for decreasing z . *Right b:-* The wave sequence $\mathcal{H}_1, \mathcal{R}_1$ and \mathcal{C}_1 in $\mathcal{W} - II$.

For $I = (z_i, t_i) \in I$, the wave sequence is as in Fig. 8.a. There is a shock curve \mathcal{S}_1 and a rarefaction \mathcal{R}_1 . Since in region I the rarefaction crosses from slow region to fast region (changing from slow rarefaction to fast rarefaction) the rarefaction \mathcal{R}_1 touches elliptic boundary and then the rarefaction changes to \mathcal{R}_2 . Since the rarefaction \mathcal{R}_2 does not touch the inflection \mathcal{I}_f , there is no composite wave here, see Fig. 8.a.

For $I = (z_i, t_i) \in II$, the wave sequence is as in Fig. 8.b. There are a shock curve \mathcal{S}_1 and a rarefaction \mathcal{R}_1 . The rarefaction \mathcal{R}_1 is drawn to the inflection \mathcal{I}_s . From \mathcal{I}_s we draw the composite wave \mathcal{C}_1 to the straight line that represents the double contact, see Fig. 8.a

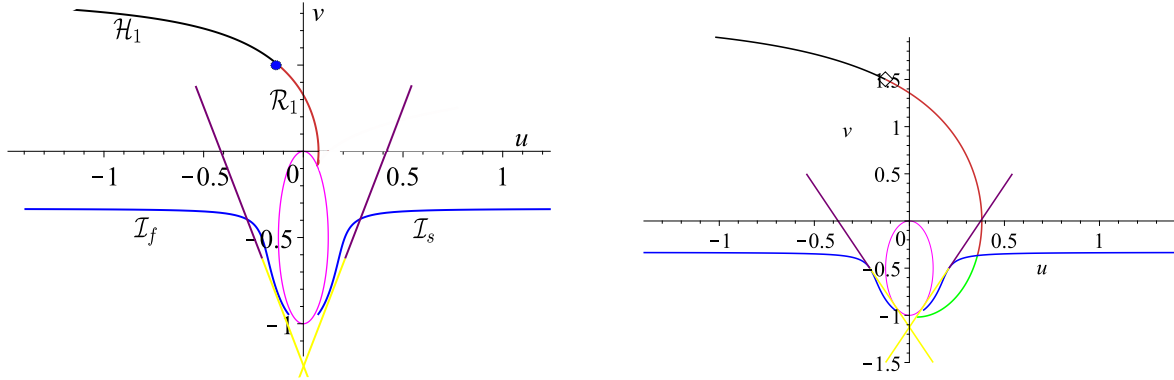


Figure 8: *Left a:)* The wave sequence for $I = (z_i, t_i) \in I$ on the plane uv . *Right b:)* The wave sequence for $I = (z_i, t_i) \in III$ on the plane uv .

For $I = (z_i, t_i) \in III$, the wave sequence is as in Fig. 9. There are a shock curve \mathcal{S}_1 and a rarefaction \mathcal{R}_1 . The rarefaction \mathcal{R}_1 is drawn to the inflection \mathcal{I}_s . From \mathcal{I}_s we draw the composite wave \mathcal{C}_1 to the straight line that represents the double contact, see Fig. 9.

9.3 The saturated surfaces

The wave curves in slow region ($t < 0$) represents on the plane uv (physical planes) waves of family 1 (shock, \mathcal{S}_1 , rarefaction, \mathcal{R}_1 and composite, \mathcal{C}_1).

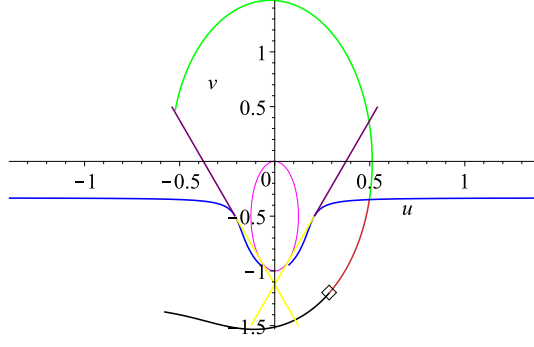


Figure 9: The wave sequence for $I = (z_i, t_i) \in III$ on the plane uv .

It is necessary to study the interaction of this family 1 with the family 2. Here in the wave manifold, the curve from the slow region ($t < 0$) should access their corresponding projection in C_f .

We know that give a state U in wave manifold \mathcal{W} , we can obtain a unique Hugoniot' through this point. Here, we are assuming that U lies in the Hyperbolic region, *i.e.*, the Hugoniot' (and Hugoniot) through U crosses \mathcal{C} in C_s and C_f .

Using the saturation of each wave, we obtain a surface that crosses C_s to C_f , as we explain as follows.

First, we consider a state $U \in C_s$. From U , we draw the wave sequence (as described in Section ??). These wave sequence defines a connected curve as we denote as C :

$$C = \{(z, t(z), Y(z)) \quad \text{such that} \quad z \in \Theta\}, \quad (9.1)$$

where is Θ is a interval.

From each point of each curve of C , we draw the Hugoniot' that crosses C_s (and C_f). So, we define the saturated of a curve C , denoted as SAT_C , as:

$$SAT_C = \left\{ \bigcup_{z \in \Theta} sh'(U) \quad \text{such that} \quad U \in C \right\}, \quad (9.2)$$

here $sh'(U)$ is the Hugoniot' through U .

In Fig. 10, we give an example of a sequence of waves, starting at state $U \in C_s$. In Fig. 10.a, the yellow curve is a rarefaction to the inflection curve. From the inflection there is a blue curve, that is the composite wave. In Fig. 10.b, in other view, we can see the shock curve from the same state U .

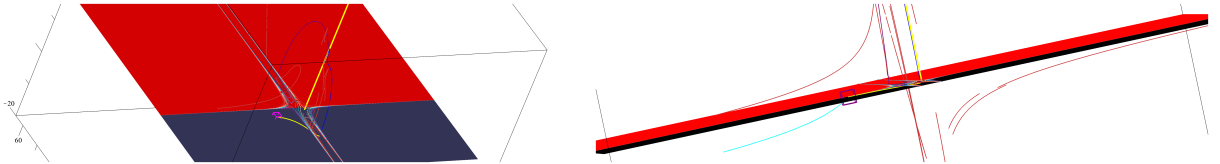


Figure 10: *Left a:)*The wave sequence from a state $U \in C_s$ the yellow curve represents a rarefaction and the blue is a composite wave. *Right b:)* From other view we can see the shock curve from U .

To access C_s , we saturated each wave. The saturated of rarefaction is the brown surface drawn in Fig. 11.a; the saturated of shock is the magenta surface drawn in Fig. 11.b; the saturated of composite is the green surface drawn in Fig. 12.a. In Fig. 12.b, we drawn are saturated together.

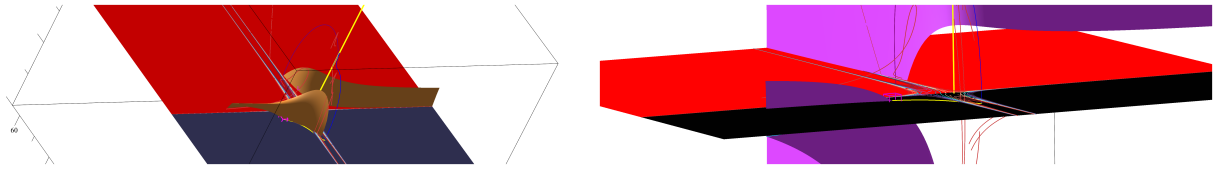


Figure 11: *Left a:)* The saturated of rarefaction wave. *Right b:)* The saturated of shock wave.

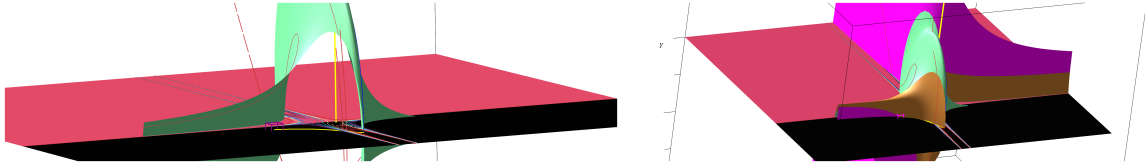


Figure 12: *Left a:)* The saturated of composite wave. *Right b:)* All saturated put together.

9.4 2-reverse wave sequence

To obtain the Riemann solution we need to construct the wave in the backward direction. We define the backward direction through 2-reverse shock. We will show that this 2-reverse shock, in following the direction from left to right is a Lax's 2-shock, satisfying conditions (6.3), so, we define the rarefaction (and composite waves) in the opposite direction.

For a state $U \in \mathcal{C}_f$, we define the 2-reverse shock as the arc of Hugoniot for which the shock speed increases along of this arc. The rarefaction is constructed in the opposite direction. Following this construction and remembering that Fig. ??, we have that the reverse rarefaction is drawn in the direction of \mathcal{I}_f and the Hugoniot is drawn in the opposite direction as in Fig. 13.

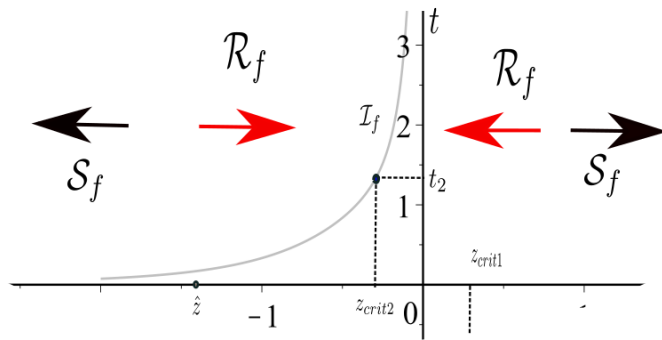


Figure 13: Direction of reverse waves in \mathcal{C}_f .

We prove now that the reverse 2-shock satisfies the Lax's condition (6.3).

First, we consider $\tilde{U} \in \mathcal{C}_f$. From \tilde{U} we draw the Hugoniot, that we denote as $sh(\tilde{U})$ and consider the arc for which shock speed increases as $sh^+(U)$. Let $U \in sh^+(\tilde{U})$ and close to \tilde{U} . Notice that since we are constructing the reverse 2-shock, we have that for the direct wave $U \in sh^+(\tilde{U})$ represents the "left" state and \tilde{U} the "right". Since the shock speed increasing s in the reverse 2-shock, follows that

$$s(U) > s(\tilde{U}) = \lambda_f(U), \quad (9.3)$$

that is the first inequality in (6.3).

To prove the other inequality of (6.3), we use the following assumption proved in [1]:

Assumption 9.1. *Let $\mathcal{V} \in \mathcal{W}$ be a neighborhood of a point $\mathcal{U} \in \mathcal{C}$ away from the inflection and the coincidence loci. Let \mathcal{V}_1 be one of the two connected components of $\mathcal{V} - \mathcal{C}$. In this paper we assume that if s decreases along the Hugoniot curve through \mathcal{U} into \mathcal{V}_1 , then s increases along the Hugoniot' curve through \mathcal{U} into \mathcal{V}_1 . A similar statement is assumed to hold if s increases along the Hugoniot curve into \mathcal{V}_1 .*

Now, to prove the second inequality in (6.3), we need to obtain the projection of $U \in sh^+(\tilde{U})$ into \mathcal{C}_s to obtain the values of λ_s evaluated in these projections. To do, we define U_s , U_f , U'_s and U'_f to be the points satisfying (6.1). Notice that to reach \tilde{U} the shock speed decreases, thus, from the Assumption 9.1, the shock speed along of Hugoniot' increases to reach U_f , so, we know that

$$s(U) < s(U'_f) = \lambda_f(U'_f) \quad (9.4)$$

Finally, to reaches the projection U'_s , we follows the opposite direction of the arc of Hugoniot' that reaches U'_f , thus the shock speed decreases along of this curve, so, we have that:

$$\lambda_s(U') = s(U') < s(U). \quad (9.5)$$

Using (9.3), (9.4) and (9.5), we have that the shock satisfies the Lax's condition (6.3) and it is a Lax's 2-shock and the proof is completed.

Remark 7. *In [1], authors proved that the shock satisfies the Lax's conditions, i.e., the shock is either 1-shock of Lax or a 2-shock of Lax. However, in the paper [1], to prove that the shock from for a state in \mathcal{C}_s is a 1-shock, authors consider $U \in \mathcal{C}_s$, as a abuse in notation they consider another state that belongs to 1-shock curve that they also call as \mathcal{U} . Despite the abuse of notation, they correctly proved that the shock is a 1-shock. A similar abuse of notation appears to consider that the 2-reverse shock is satisfies the Lax's condition (6.3). In the present paper, we corrected these mistakes and we gave details of the proof that the 2-reverse shock satisfies the Lax's conditions (6.3).*

In the following examples we show the Riemann solution in the wave manifold \mathcal{W} and the corresponding solution in uv -plane.

9.5 Examples of solutions

Example 1.

First, we consider a state $W_L = (u_L, v_L)$ for which the state \mathcal{U}_L (obtained by Algorithm RS) belongs to I .

Applying the Algorithm RS, we construct the waves of family-1 through W_L . For this example, we consider, see Fig 15.a.

In this example, we utilize $z_L = -5$ and $t_L = -0.065$ (the corresponding value in the uv plane is $u_L = -0.2430769231$ and $v_L = -0.6365384615$). The sequence through \mathcal{U}_L is $\mathcal{H}_1\mathcal{U}_L\mathcal{R}_1$ and the curve stops at the coincidence curve. Notice that in this sequence, the rarefaction curve (\mathcal{R}_1) crosses \mathcal{C}_s at $t = 0$, see Figs. 14 (in wave manifold \mathcal{W}) and 15.a in the uv -plane.

The saturated curves are described also in Fig. 14. The magenta surface is the saturated of \mathcal{H}_1 ; the brown surface is the saturated of \mathcal{R}_1 and \mathcal{R}_2 ; the green surface is the saturated of \mathcal{C}_2 . The curve \mathcal{C}_2 is drawn to reach the double contact in $z = 1/3$.

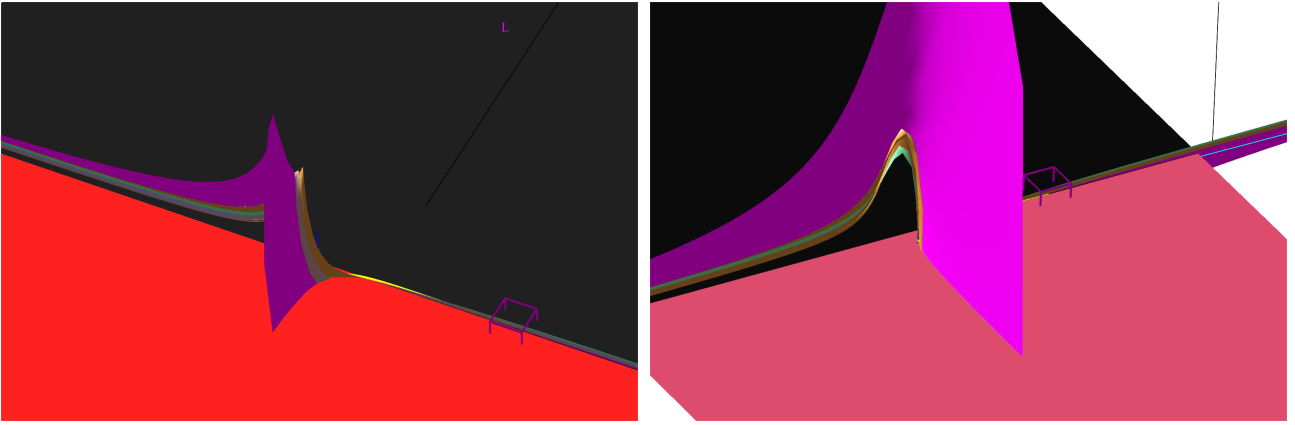


Figure 14: The wave sequence and the saturated surface from \mathcal{U}_L in region I , here $z_L = -5$ and $t_L = -0.065$. From \mathcal{U}_L , denoted as a magenta box, we have the wave sequence $\mathcal{H}_1\mathcal{U}_L\mathcal{R}_1$. The magenta surface is the saturated of \mathcal{H}_1 ; the brown surface is the saturated of \mathcal{R}_1 and \mathcal{R}_2 ; the green surface is the saturated of \mathcal{C}_2 . The curve \mathcal{C}_2 is drawn to reach the double contact in $z = 1/3$.

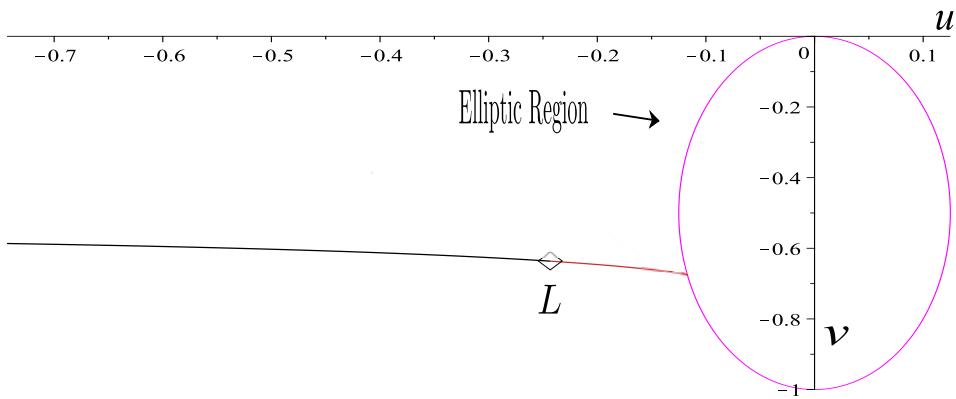


Figure 15: The wave sequence on the plane uv , here $u_L = -0.2430769231$ and $v_L = -0.6365384615$. From L there is a \mathcal{H}_1 (black curve) and a \mathcal{R}_1 (red curve).

To construct the 2-reverse wave sequence, here we have two possibilities.

The first possibility, we give $(z_R = 2, t_R = 2) \in \mathcal{C}_f$ (the corresponding values on the plane uv are $(u_R = 0.8500000000, v_R = 3.2000000000)$). From \mathcal{U}_r (obtained as described in Algorithm RS) we draw the 2-reverse wave sequence that is given by $\mathcal{H}_2\mathcal{U}_R\mathcal{R}_2\mathcal{C}_2$, as described in Fig. 16. In the wave manifold \mathcal{W} , \mathcal{R}_2 is the green curve and \mathcal{C}_2 is the black curve, the \mathcal{H}_2 is below \mathcal{C}_f . Notice that, from Fig. 16.a, that \mathcal{C}_2 crosses the saturated of \mathcal{H}_1 (the magenta surface) in a state in \mathcal{W} .

The Riemann solution from state \mathcal{U}_L consists of a \mathcal{H}_1 from \mathcal{U}_L to state \mathcal{U}_M ; from \mathcal{U}_M there is a \mathcal{C}_2 (a right characteristic shock) followed by a \mathcal{R}_2 to \mathcal{U}_R . The solution in \mathcal{W} is described in Fig. 16.a and in the uv plane is described in 16.b.

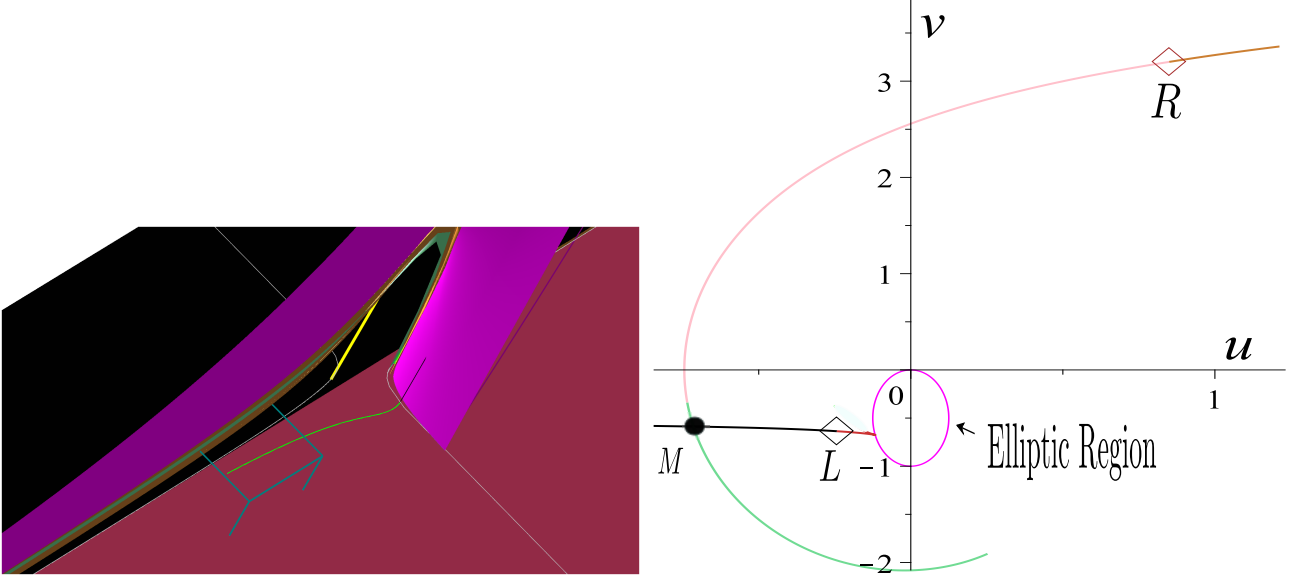


Figure 16: The Riemann solution from state \mathcal{U}_L consists of a \mathcal{H}_1 from \mathcal{U}_L to state \mathcal{U}_M ; from \mathcal{U}_M there is a \mathcal{C}_2 (a right characteristic shock) followed by a \mathcal{R}_2 to \mathcal{U}_R . *Left- a:)* The solution in the wave manifold \mathcal{W} . *Right- b:)* The Riemann solution in plane uv , for $L = (u_L = -0.2430769231, v_L = -0.6365384615)$ and $R = (u_R = -0.85, v_R = 3.2)$.

In the second possibility for \mathcal{U}_R , we give $(z_R = 0.385677655, t_R = 4.849940052) \in \mathcal{C}_f$ (the corresponding values on the plane uv are $(u_R = -0.6, v_R = -1.1)$). From \mathcal{U}_r (obtained as described in Algorithm RS) we draw the 2-reverse wave sequence that is given by $\mathcal{C}_2\mathcal{R}_2\mathcal{U}_R\mathcal{H}_2$, as described in Fig. 17. In the wave manifold \mathcal{W} , \mathcal{R}_2 is the green curve, \mathcal{H}_2 is the blue curve and \mathcal{C}_2 is below \mathcal{C}_f . Notice that, from Fig. 17.a, that \mathcal{R}_2 crosses the saturated of \mathcal{H}_1 (the magenta surface) in a state in \mathcal{W} .

The Riemann solution from state \mathcal{U}_L consists of a \mathcal{H}_1 from \mathcal{U}_L to state \mathcal{U}_M ; from \mathcal{U}_M there is a \mathcal{R}_2 to \mathcal{U}_R . The solution in \mathcal{W} is described in Fig. 17.a and in the uv plane is described in 17.b.

Example 2.

In this example we utilize $z_L = 1$ and $t_L = -1$ (the corresponding value in the uv plane is $u_L = 0.125, v_L = 0.5$), the state (z_L, t_L) belongs also to the region I . The sequence through \mathcal{U}_L is $\mathcal{H}_1\mathcal{U}_L\mathcal{R}_1$, there is no composite wave because the rarefaction does not reach the inflection curve. However, notice that, the rarefaction curve (\mathcal{R}_1) crosses \mathcal{C}_s at $t = 0$ and the wave curve stops, see Figs. 18 (in wave manifold \mathcal{W}) and 19 in the uv -plane.

The saturated curves are described also in Fig. 19. The magenta surface is the saturated of \mathcal{H}_1 ; the brown surface is the saturated of \mathcal{R}_1 and \mathcal{R}_2 .

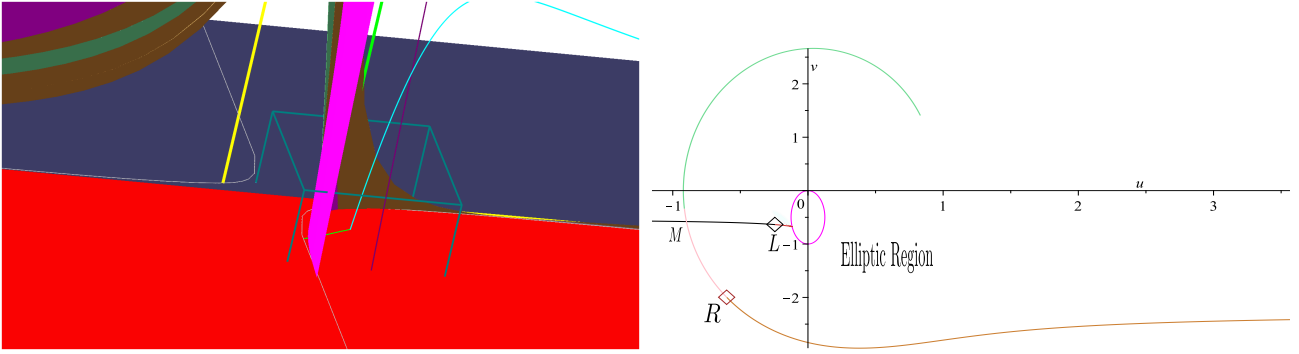


Figure 17: The 2-reverse wave sequence that is $C_2\mathcal{R}_2\mathcal{U}_R\mathcal{H}_2$. The Riemann solution from state \mathcal{U}_L consists of a \mathcal{H}_1 from \mathcal{U}_L to state \mathcal{U}_M ; from \mathcal{U}_M there is a \mathcal{R}_2 to \mathcal{U}_R . *Left- a:)* The solution in the wave manifold \mathcal{W} , here \mathcal{R}_2 is the green curve, \mathcal{H}_2 is the blue curve and C_2 is below C_f . *Right- b:)* The Riemann solution in plane uv , for $L = (u_L = -0.2430769231, v_L = -0.6365384615)$ and $R = (u_R = -0.6, v_R = -1.1)$.

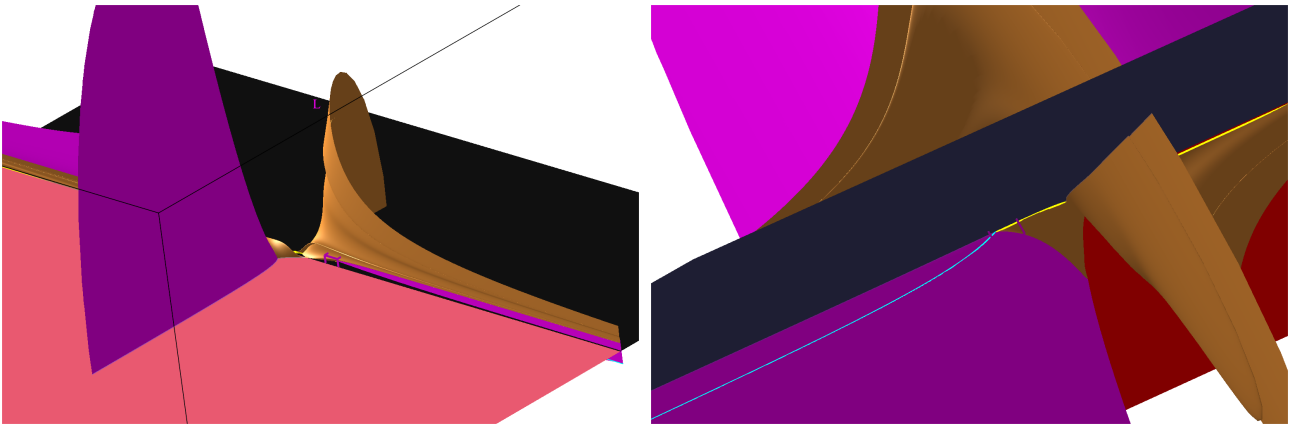


Figure 18: The wave sequence and the saturated surface from \mathcal{U}_L in region II , here $z_L = 1$ and $t_L = -1$. From \mathcal{U}_L , denoted as a magenta box, we have the wave sequence $\mathcal{H}_1\mathcal{U}_L\mathcal{R}_1\mathcal{R}_2$. The magenta surface is the saturated of \mathcal{H}_1 and the brown surface is the saturated of \mathcal{R}_1 and \mathcal{R}_2 ; there is no composite wave, because the rarefaction does not reach the inflection curve. Here, we have different views of the \mathcal{U}_L . *Left- a:)* The view for $Y > 0$. *Right- b:)* The view with $Y < 0$ the blue curve represents \mathcal{H}_1 and yellow is \mathcal{R}_1 .

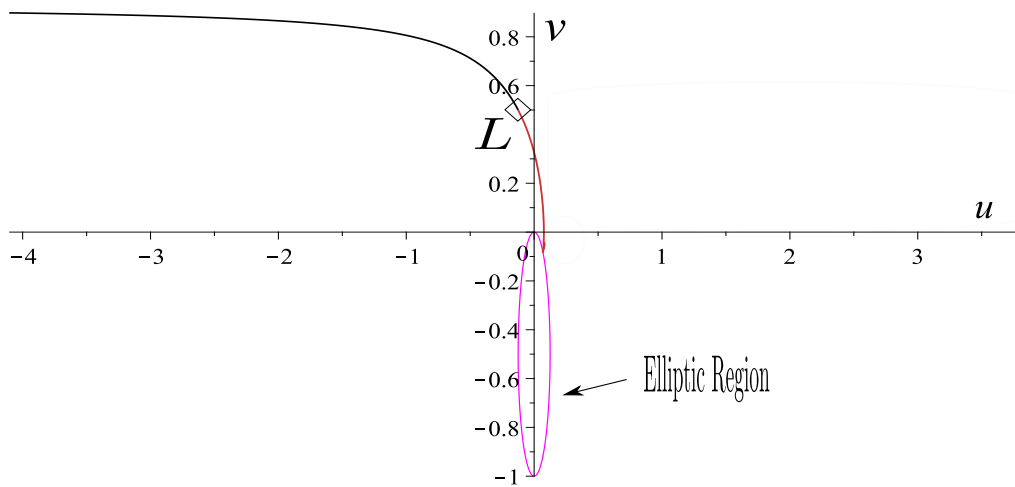


Figure 19: The wave sequence on the plane uv , here $u_L = 0.125$ and $v_L = 0.5$. From L there is a \mathcal{H}_1 (black curve) and a \mathcal{R}_1 (red curve). The magenta ellipse is the elliptic region.

To construct the 2-reverse wave sequence, we consider \mathcal{U}_r (obtained as described in Algorithm RS) and we draw the 2-reverse wave sequence that is given, in this example, by $\mathcal{C}_2\mathcal{R}_2\mathcal{U}_R\mathcal{H}_2$, as described in Fig. 16. In the wave manifold \mathcal{W} , \mathcal{R}_2 is the green curve on the plane \mathcal{C}_f and \mathcal{C}_2 is the black curve for $Y < 0$ (below \mathcal{C}_f , the \mathcal{H}_2 is the blue curve for $Y < 0$ (above \mathcal{C}_f). Notice that, from Fig. 20.a, that \mathcal{C}_2 crosses the saturated of \mathcal{H}_1 (the magenta surface) in a state in \mathcal{W} for $Y < 0$ (below \mathcal{C}_f).

The Riemann solution from state \mathcal{U}_L consists of a \mathcal{H}_1 from \mathcal{U}_L to state \mathcal{U}_M ; from \mathcal{U}_M there is a \mathcal{C}_2 (a right characteristic shock) followed by a \mathcal{R}_2 to \mathcal{U}_R . The solution in \mathcal{W} is described in Fig. 20 and in the uv plane is described in Fig. 21.

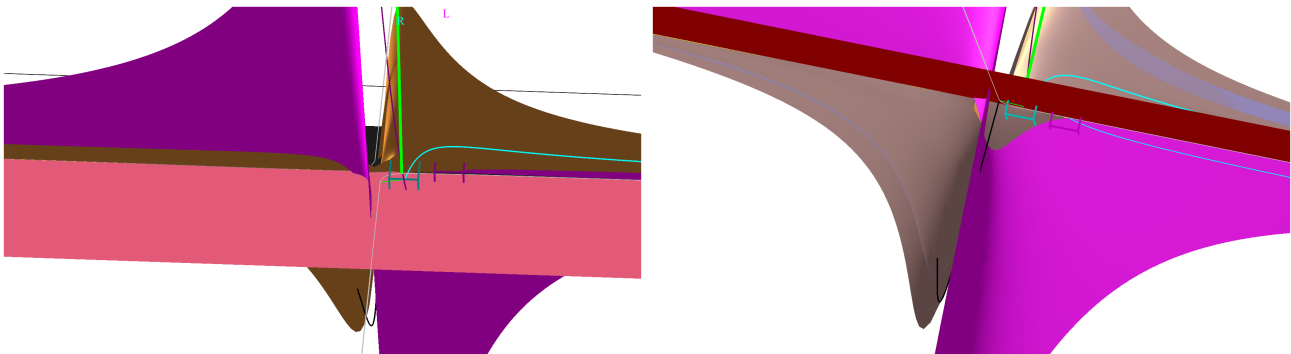


Figure 20: The 2-reverse wave sequence that is $\mathcal{C}_2\mathcal{R}_2\mathcal{U}_R\mathcal{H}_2$. The green curve on the plane \mathcal{C}_f and \mathcal{C}_2 is the black curve for $Y < 0$ (below \mathcal{C}_f , the \mathcal{H}_2 is the blue curve for $Y < 0$ (above \mathcal{C}_f). Notice that \mathcal{C}_2 crosses the saturated of \mathcal{H}_1 (the magenta surface) in a state in \mathcal{W} for $Y < 0$ (below \mathcal{C}_f).

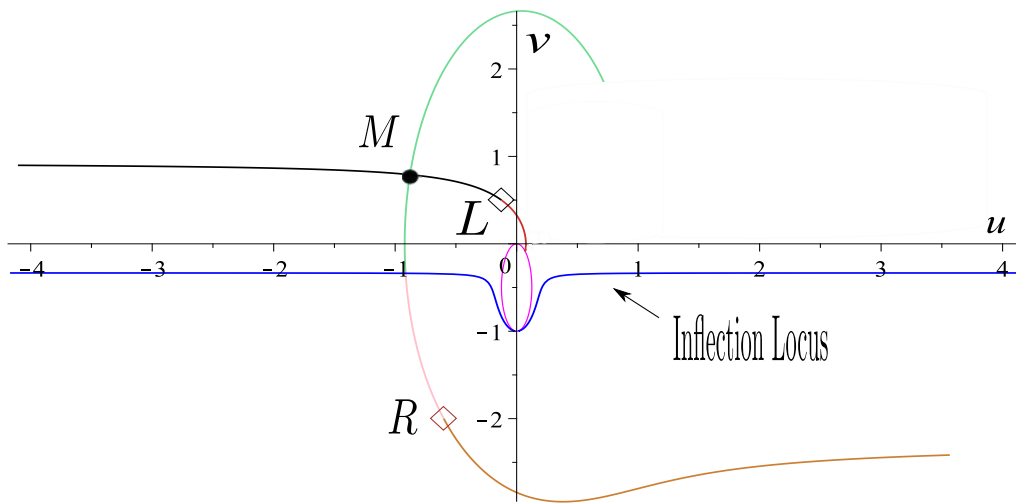


Figure 21: The Riemann solution in plane uv , for $L = (u_L = -0.125, v_L = 3.5)$ and $R = (u_R = -0.75, v_R = -2.5)$. From state L consists of a \mathcal{H}_1 from L to state M ; from M there is a \mathcal{C}_2 (a right characteristic shock) followed by a \mathcal{R}_2 to R .

Example 3.

In this example, we utilize $z_L = -1$ and $t_L = -4$ (the corresponding value in the uv plane is $u_L = -0.125, v_L = 3.5$), the state (z_L, t_L) belongs to the region II . The sequence through \mathcal{U}_L is $\mathcal{H}_1\mathcal{U}_L\mathcal{R}_1\mathcal{C}_1$, see Figs. 22 (in wave manifold \mathcal{W}) and 19 in the uv -plane.

In Fig. 22, the magenta surface is the saturated of \mathcal{H}_1 ; the brown surface is the saturated of \mathcal{R}_1 and \mathcal{R}_2 ; the green surface is the saturated of \mathcal{C}_2 . The curve \mathcal{C}_2 is drawn to reach the double contact in $z = -1/3$.

In Fig. 23, the double contact $z = -1/3$ is the yellow straight line.

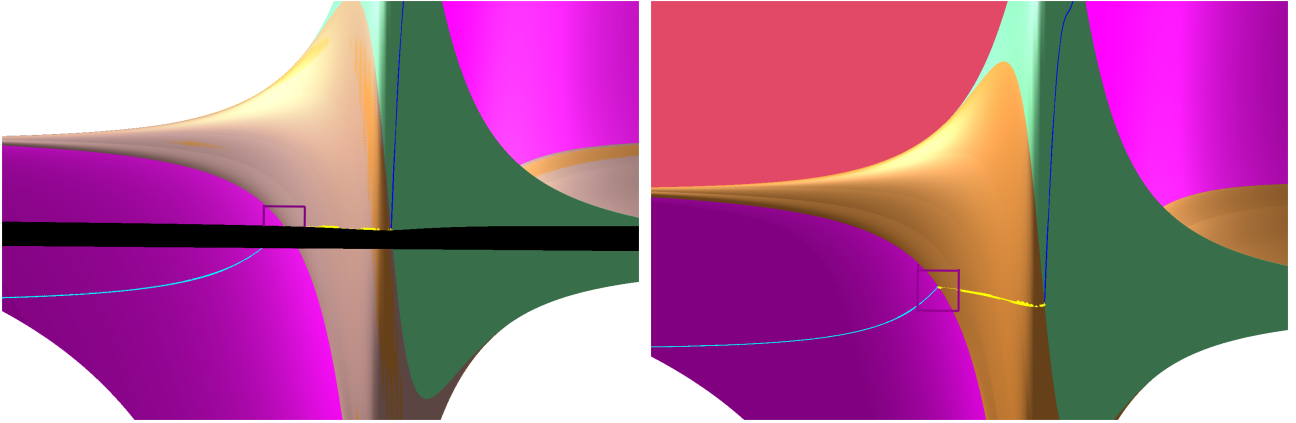


Figure 22: Here the values for \mathcal{U}_L in *III* with $z_L = -1$ and $t_L = -4$. The sequence through \mathcal{U}_L is $\mathcal{H}_1\mathcal{U}_L\mathcal{R}_1\mathcal{C}_1$. The magenta surface is the saturated of \mathcal{H}_1 (blue curve); the brown surface is the saturated of \mathcal{R}_1 (yellow curve); the green surface is the saturated of \mathcal{C}_2 (cyan). The curve \mathcal{C}_2 is drawn to reach the double contact in $z = -1/3$.

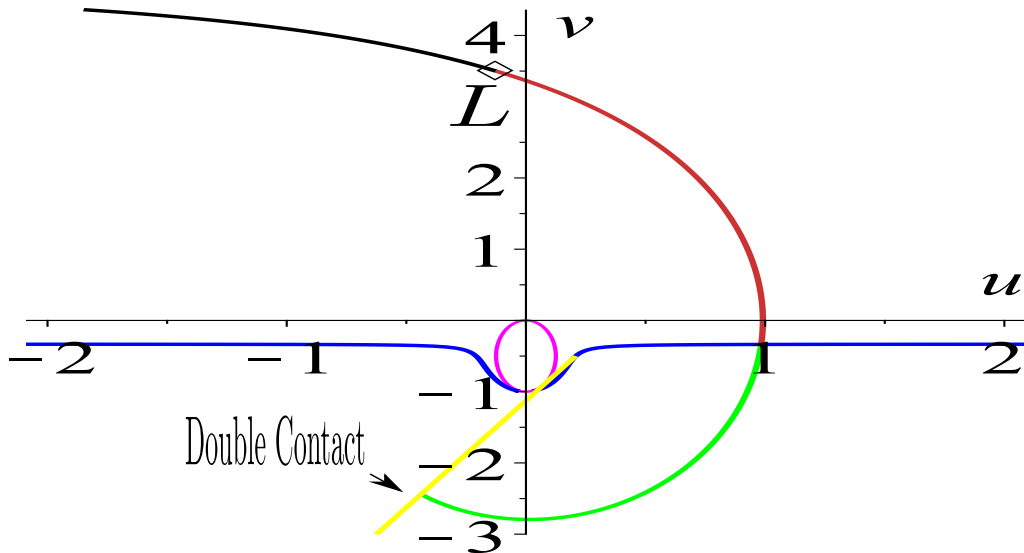


Figure 23: The wave sequence on the plane uv , here $u_L = -0.125$ and $v_L = 3.5$. From L there is a \mathcal{H}_1 (black curve) and a \mathcal{R}_1 (red curve), since the rarefaction crosses the inflection (blue curve), there is a \mathcal{C}_2 to the double contact (yellow straight line) $z = -1/3$. The magenta ellipse is the elliptic region.

To construct the 2-reverse wave sequence, here we consider $(z_R = 5, t_R = 3) \in \mathcal{C}_f$ (the corresponding values on the plane uv are $(u_R = 9.048076925, v_R = 14.03846154)$). From \mathcal{U}_r (obtained as described in Algorithm RS) we draw the 2-reverse wave sequence that is given, in this example, by $\mathcal{H}_2\mathcal{U}_R\mathcal{R}_2\mathcal{C}_2$, as described in Fig. 24. In the wave manifold \mathcal{W} , \mathcal{R}_2 is the green curve on \mathcal{C}_f . The curve \mathcal{H}_1 is drawn for $Y < 0$, *i.e.*, below \mathcal{C}_f and \mathcal{C}_2 is the black curve behind the magenta surface (saturated of \mathcal{H}_1), from \mathcal{U}_R there is only a wave crossing the magenta surface, that is \mathcal{R}_2 .

In this case, the Riemann solution from state \mathcal{U}_L consists of a \mathcal{H}_1 from \mathcal{U}_L to state \mathcal{U}_M ; from \mathcal{U}_M there is a \mathcal{R}_2 to \mathcal{U}_R . The solution in \mathcal{W} is described in Fig. 24 and in the uv plane is described in 25.

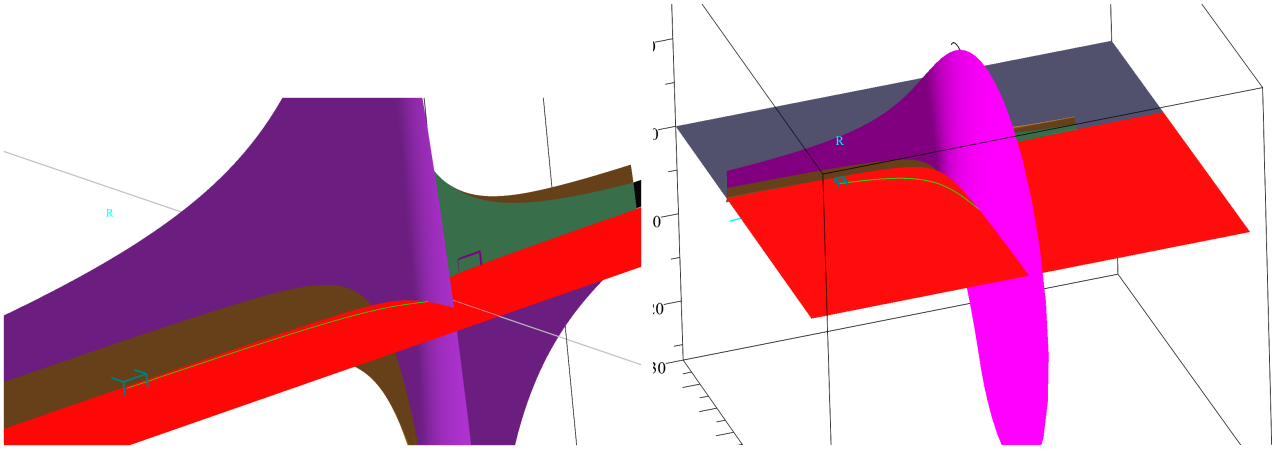


Figure 24: The 2-reverse wave sequence for $(z_R = 5, t_R = 3) \in \mathcal{C}_f$ is $\mathcal{H}_2\mathcal{U}_R\mathcal{R}_2\mathcal{C}_2$. The \mathcal{R}_2 is the green curve on \mathcal{C}_f . The curve \mathcal{H}_1 is drawn for $Y < 0$ (below \mathcal{C}_f) and \mathcal{C}_2 is the black curve behind the magenta surface. The Riemann solution from state \mathcal{U}_L consists of a \mathcal{H}_1 from \mathcal{U}_L to state \mathcal{U}_M ; from \mathcal{U}_M there is a \mathcal{R}_2 to \mathcal{U}_R .

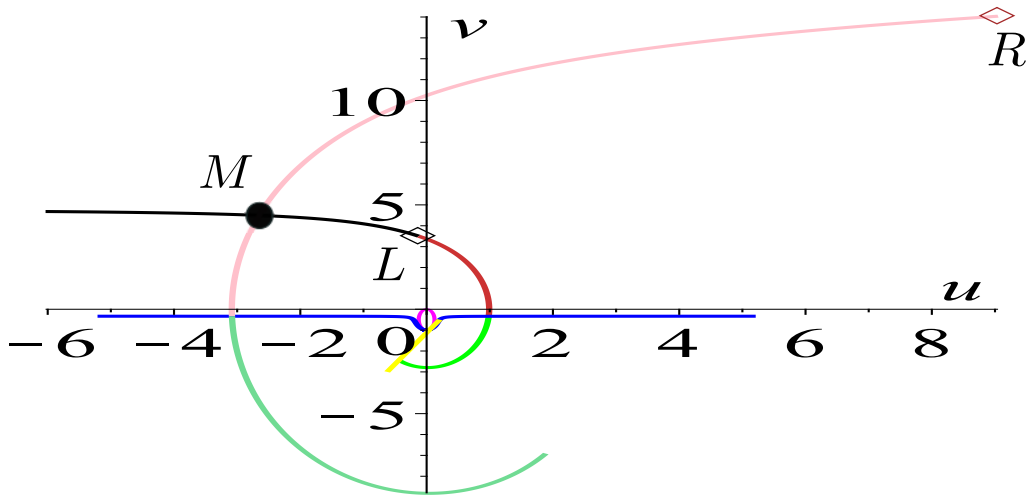


Figure 25: The Riemann solution in plane uv , for $L = (u_L = -0.125, v_L = 3.5)$ and $R = (u_R = 9.048076925, v_R = 14.03846154)$. From L there is a \mathcal{H}_1 to a state M (black curve); from M there is a \mathcal{R}_2 (pink curve) to R . The blue curve is the inflection.

Example 4.

In this example, we utilize $z_L = 1$ and $t_L = -2$ (the corresponding value in the uv plane is $u_L = 0.125, v_L = -2.5$), the state (z_L, t_L) belongs to the region III . The sequence through \mathcal{U}_L is $\mathcal{C}_1\mathcal{R}_1\mathcal{U}_L\mathcal{H}_1$, see Figs. 26 (in wave manifold \mathcal{W}) and 27 (in the uv -plane).

In Fig. 26, the magenta surface is the saturated of \mathcal{H}_1 ; the brown surface is the saturated of \mathcal{R}_1 and \mathcal{R}_2 ; the green surface is the saturated of \mathcal{C}_2 . The curve \mathcal{C}_2 is drawn to reach the double contact in $z = 1/3$ (with $t < 0$). In Fig. 27, the double contact $z = 1/3$ is the purple straight line.

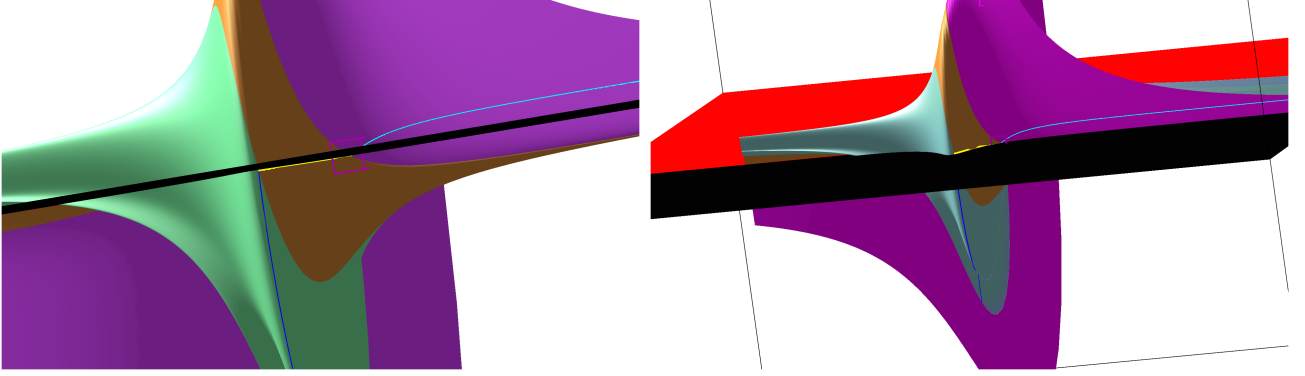


Figure 26: Here the values for \mathcal{U}_L in III with $z_L = 1$ and $t_L = -2$. The sequence through \mathcal{U}_L is $\mathcal{C}_1\mathcal{R}_1\mathcal{U}_L\mathcal{H}_1$. The magenta surface is the saturated of \mathcal{H}_1 (blue curve); the brown surface is the saturated of \mathcal{R}_1 (yellow curve); the green surface is the saturated of \mathcal{C}_2 (cyan). The curve \mathcal{C}_2 is drawn to reach the double contact in $z = 1/3$.

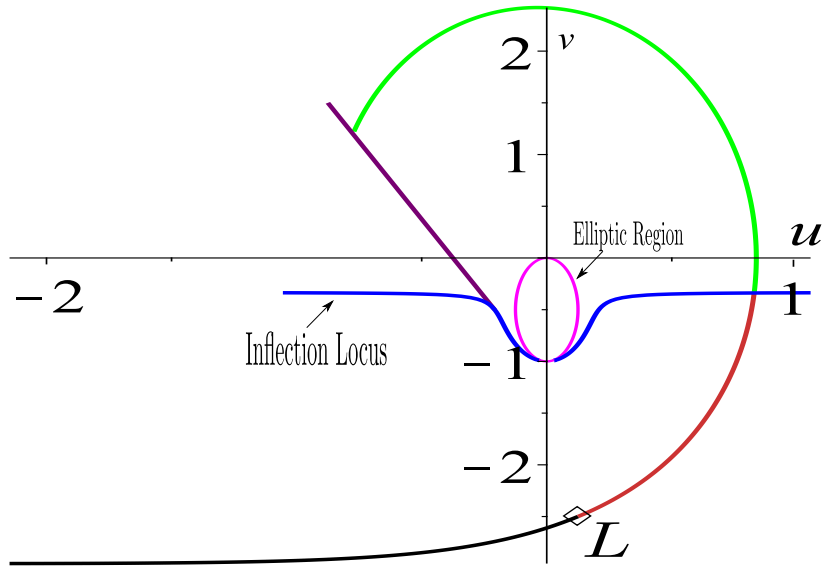


Figure 27: The wave sequence on the plane uv , here $u_L = 0.125$ and $v_L = -2.5$. From L there is a \mathcal{H}_1 (black curve) and a \mathcal{R}_1 (red curve), since the rarefaction crosses the inflection (blue curve), there is a \mathcal{C}_2 to the double contact (purple straight line) $z = 1/3$. The magenta ellipse is the elliptic region.

To construct the 2-reverse wave sequence, here we consider $(z_R = 4.961249694, t_R = 1) \in \mathcal{C}_f$ (the corresponding values on the plane uv are $(u_R = 3, v_R = 4)$). From \mathcal{U}_r (obtained as described in Algorithm RS) we draw the 2-reverse wave sequence that is given, in this example, by $\mathcal{C}_2\mathcal{R}_2\mathcal{U}_r\mathcal{H}_2$, as described in Fig. 28. In the wave manifold \mathcal{W} , \mathcal{R}_2 is the green curve on \mathcal{C}_f . The curve \mathcal{H}_1 is the cyan curve drawn for

$Y > 0$ and increasing z . The curve \mathcal{C}_2 is the black curve below \mathcal{C}_f , from \mathcal{U}_R the curve \mathcal{R}_2 crosses the saturated surface of \mathcal{C}_1 (green surface).

In this case, the Riemann solution from state \mathcal{U}_L consists of a \mathcal{R}_1 followed by a \mathcal{C}_1 to a state \mathcal{U}_M ; from \mathcal{U}_M there is a \mathcal{R}_2 to \mathcal{U}_R . The solution in \mathcal{W} is described in Fig. 28 and in the uv plane is described in Fig. 29.

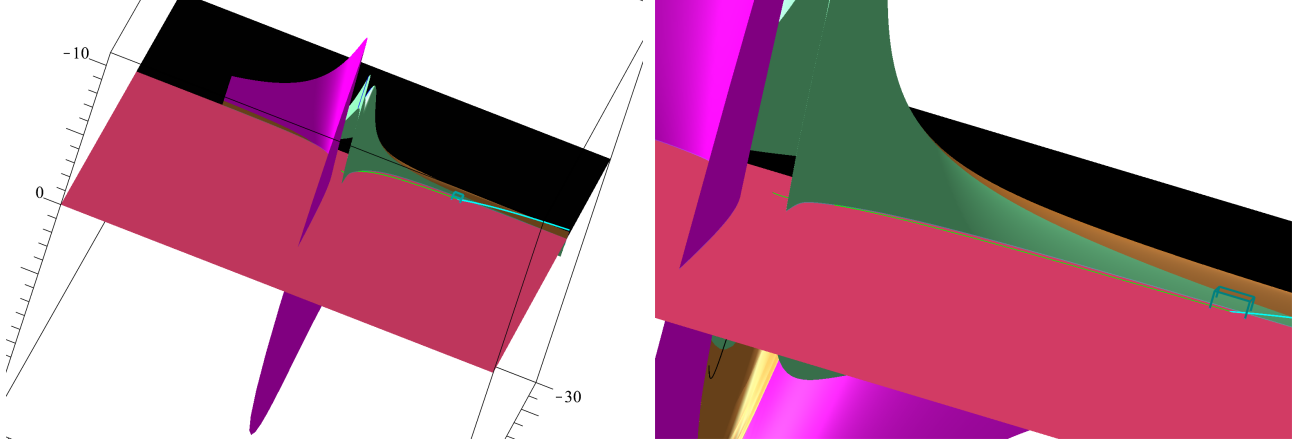


Figure 28: The 2-reverse wave sequence for $(z_R = 4.961249694, t_R = 1) \in \mathcal{C}_f$ is $\mathcal{C}_2\mathcal{R}_2\mathcal{U}_R\mathcal{H}_2$. Here \mathcal{R}_2 is the green curve on \mathcal{C}_f . The curve \mathcal{H}_1 is the cyan curve drawn for $Y > 0$ and increasing z . The curve \mathcal{C}_2 is the black curve below \mathcal{C}_f , from \mathcal{U}_R the curve \mathcal{R}_2 crosses the saturated surface of \mathcal{C}_1 (green surface). The Riemann solution from state \mathcal{U}_L consists of a \mathcal{R}_1 followed by a \mathcal{C}_1 to a state \mathcal{U}_M ; from \mathcal{U}_M there is a \mathcal{R}_2 to \mathcal{U}_R .

9.6 The Regions in Phase Space

For the flux function $f(u, v)$ and $g(u, v)$ given in equation (2.1), we can obtain the eigenpairs (eigenvalues, λ , and eigenvectors, \vec{r}) in the phase space (u, v) . These eigenpairs are solutions of:

$$\mathbf{A}\vec{r} = \lambda\vec{r}, \quad \text{where } \lambda \text{ is obtained solving } \det(\mathbf{A} - \lambda\mathbf{I}) = 0. \quad (9.6)$$

Here \mathbf{A} is the jacobian of $(f, g)^\top$ and \mathbf{I} is the 2×2 identity matrix. Notice that from equation (9.6.b) we have a degree two polynomial, thus for each state (u, v) in the phase space we have associated two eigenvalues λ . The phase space is classified using λ and \vec{r} . The region in the phase space (u, v) for which each state admits two real eigenvalues λ and a basis of eigenvectors (local) is called *hyperbolic region*, which we denote as \mathcal{R}_H . The region for which we have complex (and conjugated) eigenvalues λ is called *elliptic region*, denoted as \mathcal{R}_E . The boundary (if this boundary exists) between \mathcal{R}_H and \mathcal{R}_E is denoted as $\partial\mathcal{R}_E$, here the two eigenvalues are equals.

For $f(u, v)$ and $g(u, v)$ given in equation (2.1) the eigenvalues are:

$$\lambda_1 = \frac{\alpha_1 - \sqrt{\alpha_2}}{2} \quad \text{and} \quad \lambda_2 = \frac{\alpha_1 + \sqrt{\alpha_2}}{2}, \quad \text{where } \alpha_1 = u(b_1 + 2) + a_1 + a_4 \quad \text{and} \quad (9.7)$$

$$\alpha_2 = a_1^2 + (2b_1u - 2a_4)a_1 + a_4^2 - 2a_4b_1u + b_1^2u^2 + 4(v + a_2)(a_3 + v) \quad (9.8)$$

To obtain \mathcal{R}_H , \mathcal{R}_E and $\partial\mathcal{R}_E$, we need to study the signal of α_2 . After some algebraic, we can write α_2

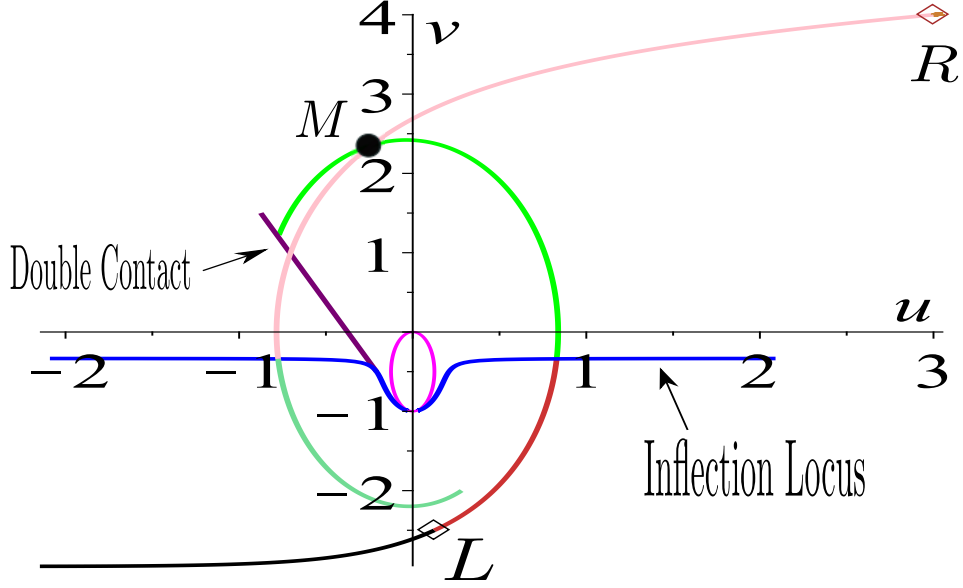


Figure 29: The Riemann solution in plane uv , for $L = (u_L = 0.125, v_L = -2.5)$ and $R = (u_R = 3, v_R = 4)$. From L there is a \mathcal{R}_1 (red curve) followed by a \mathcal{C}_1 (green curve) to state M (black curve); from M there is a \mathcal{R}_2 (pink curve) to R . The blue curve is the inflection. The purple is the double contact that corresponds to $z = 1/3$.

and define $\tilde{\alpha}_2$ as:

$$\alpha_2 = (2v + a_2 + a_3)^2 + (b_1 u + a_1 - a_4)^2 - c^2, \quad \tilde{\alpha}_2 = \frac{[v + \frac{a_2 + a_3}{2}]^2}{(\frac{c}{2})^2} + \frac{[u + \frac{a_1 - a_4}{b_1}]^2}{(\frac{c}{b_1})^2} - 1. \quad (9.9)$$

Here, we use that $c = a_3 - a_2 > 0$. From $\tilde{\alpha}_2$, we can define:

$$\mathcal{R}_H = \{(u, v) / \tilde{\alpha}_2 > 0\}, \quad \mathcal{R}_E = \{(u, v) / \tilde{\alpha}_2 < 0\} \text{ and } \partial\mathcal{R}_E = \{(u, v) / \tilde{\alpha}_2 = 0\}. \quad (9.10)$$

Notice that $\partial\mathcal{R}_E$ represents an ellipse. In Fig. 30.a, we illustrate \mathcal{R}_H , \mathcal{R}_E and $\partial\mathcal{R}_E$ for particular values of a_1, a_2, a_3, a_4, c and b_1 described in caption of figure.

From the variables change defined Section 2, we obtain u, v, u' and v' as function of Y, t and z . The variables u and v are:

$$u = \frac{2t(z^4 - 1) + Yb_1z^3 + (-2a_1 + 2a_4)(z^2 + 1) + (Yb_1 + 4c)z}{2(z^2 + 1)b_1}, \quad (9.11)$$

$$(9.12)$$

$$v = \frac{2tz^3 + (Y - 2a_3)z^2 + 2tz + Y - 2a_2}{2z^2 + 2} \quad (9.13)$$

to obtain u' and v' we use u and v interchanging Y with $-Y$.

Substituting in α_2 , u and v given equations (9.11), (9.13), we obtain an expression that we denote

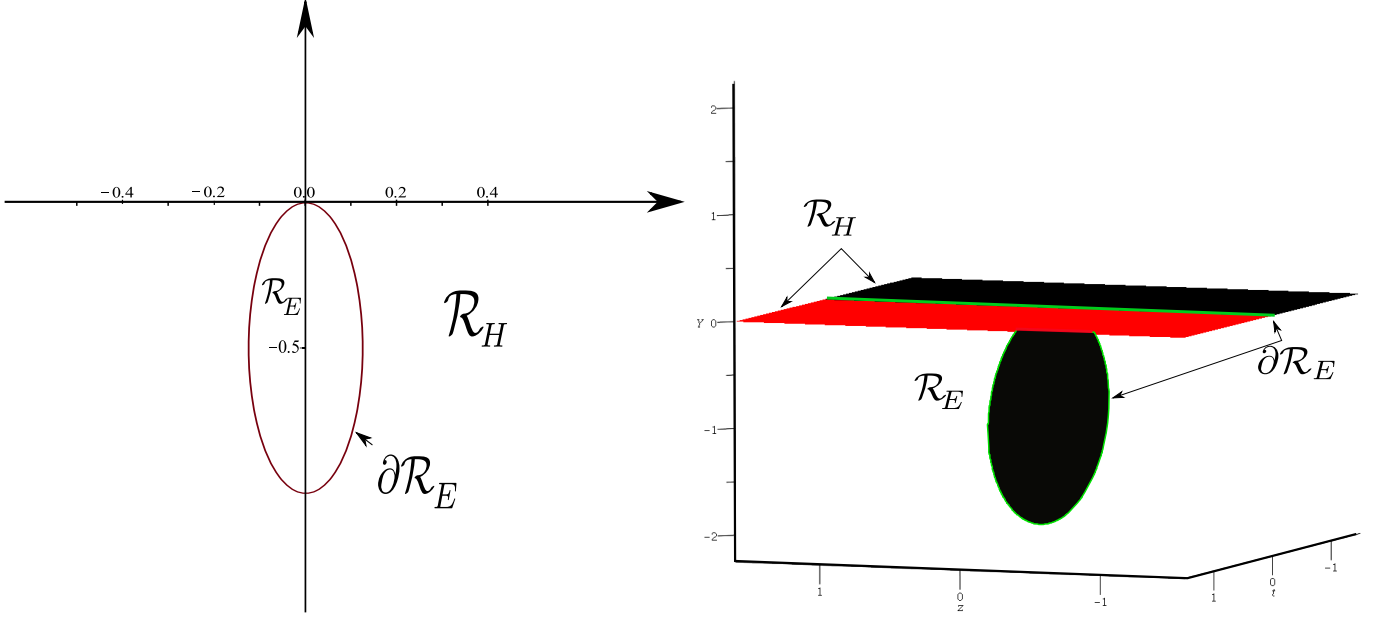


Figure 30: *Left - a:).* Regions \mathcal{R}_E , \mathcal{R}_H and the boundary $\partial\mathcal{R}_E$. Here we use $a_1 = 0$, $a_2 = 0$, $a_3 = 1$, $a_4 = 0$, $c = 1$, and $b_1 = 8$.

as $\alpha_M(Y, t, z)$:

$$\alpha_M(Y, t, z) = \frac{(Y^2 b_1^2 + 12t^2)z^4 + 16Ytz^3 + [(b_1^2 + 4)Y^2 + 8c(b_1 - 1)Y + 4c^2 + 12t^2 - 4c]z^2}{4z^2 + 4} + \frac{4t^2 z^6 + 4Yb_1 t z^5 - 4t(b_1 - 4)Yz + 4Y^2 + 8Yc + 4c^2 + 4t^2 - 4c}{4z^2 + 4}. \quad (9.14)$$

If we set $\alpha_M = 0$, we obtain the extension of \mathcal{R}_E in \mathcal{W} , which we will call *coincidence surface*, i.e.,

$$\text{coincidence} = \{(z, t, Y) / \alpha_M = 0\}. \quad (9.15)$$

Similarly, we define *coincidence'* that is obtained substituting u' and v' in α_2 . This expression is denoted as $\alpha'_M = \alpha_M(z, t, -Y)$, thus $\text{coincidence}' = \{(z, t, Y) / \alpha'_M = 0\}$. In Fig. 31, we show *coincidence surface* and the characteristic \mathcal{C} . The *coincidence'* surface is the symmetric projection of the coincidence surface in \mathcal{C} .

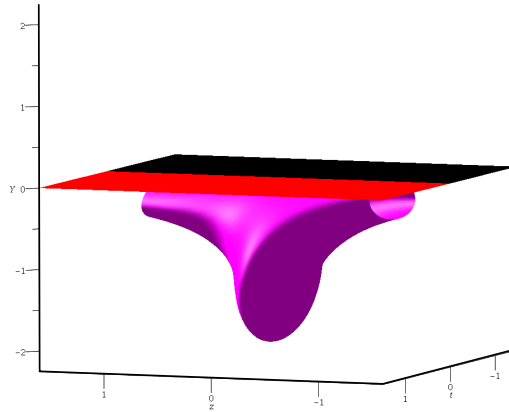


Figure 31: *Left - a:).* Regions \mathcal{R}_E , \mathcal{R}_H and the boundary $\partial\mathcal{R}_E$. Here, we use $a_1 = 0$, $a_2 = 0$, $a_3 = 1$, $a_4 = 0$, $c = 1$, and $b_1 = 8$.

Appendix

1 Characterizing the L2 Condition

In this appendix section, we will prove that the necessary and sufficient condition to verify the condition **L2** is that $z^2 < 1/(b_1 + 1)$.

As in Section 2.1, parametric equations for the Hugoniot' curve through a point (t_0, z_0, Y_0) is given by

$$\begin{cases} Y = \frac{A'z^2 + B'z + C'}{(z_0^2 + 1)[(b_1 - 1)z^2 + 1]} \\ t = \frac{D'z^3 + E'z^2 + F'z + G'}{c(z_0^2 + 1)[(b_1 - 1)z^4 + b_1z^2 + 1]}, \end{cases} \quad (1.1)$$

where $A', B', C', D', E', F', G'$ are obtained from equations (2.12) by changing Y into $-Y$ and Y_0 into $-Y_0$.

Parametric equations for Hugoniot' curve through a point of Son' are obtained from the equations (1.1) substituting t_0 by t'_0 , t'_0 as in Section 5, getting $(Y_{hug'}(z), t_{hug'}(z))$.

We need to calculate the speed s at the intersections points of the Hugoniot' curve with \mathcal{C} and then write the condition **L2**. As the inequalities involved change only in Son , it is enough to verify them at a point of Son' . The speed s at the point (t'_0, z_0, Y_0) is given by the equation (5.1).

Let z_1 and z_2 be, $z_1 < z_2$, the solutions of the equation $Y_{hug'} = 0$. The roots z_1 and z_2 are the z coordinates of the intersection points of the Hugoniot' curve with \mathcal{C} . The speed, $s_{hug'}(z)$, along the Hugoniot' curve through (t'_0, z_0, Y_0) is obtained by changing t into $t_{hug'}(z)$ in equation (2.9). We must compare the values $s_{hug'}(z_1)$ and $s_{hug'}(z_2)$ with $s_{son'}$. Denoting by $s_{hug'n}(z)$ the numerator of $s_{hug'}(z)$, $s_{hug'd}(z)$ the denominator of $s_{hug'}(z)$ and $Y_{hug'n}(z)$ the numerator of $Y_{hug'}(z)$, we can write

$$s_{hug'n}(z) = p_1(z)Y_{hug'n}(z) + r_1(z)$$

and

$$s_{hug'd}(z) = p_2(z)Y_{hug'n}(z) + r_2(z).$$

It follows that, $s_{hug'c}(z)$, given by

$$s_{hug'c}(z) = \frac{r_1(z)}{r_2(z)},$$

has the same value of $s_{hug'}(z)$ at the intersection points of the Hugoniot' curve through (t'_0, z_0, Y_0) with \mathcal{C} . The expression of $s_{hug'c}(z)$ is of the form $(az + b)/(cz + d)$. Our goal is to get a condition such that $s_{son'}(t'_0, z_0, Y_0)$ satisfies $s_{hug'c}(z_1) < s_{son'}(t'_0, z_0, Y_0) < s_{hug'c}(z_2)$.

In a more general way, we have the following problem: given a number s we want a condition such that

$$\frac{az_1 + b}{cz_1 + d} < s < \frac{az_2 + b}{cz_2 + d},$$

where z_1 and z_2 are the roots of the polynomial $fz^2 + gz + h$. Straightforward computations give that

the condition is

$$\frac{(c^2 h - dcg + d^2 f)s^2 + [agd + bcg - 2(ach + bdf)]s + a^2 h - abg + b^2 f}{c^2 h - dcg + d^2 f} < 0.$$

Changing a , b into the coefficients of the numerator of $s_{hug'c}(z)$, c and d into the coefficients of the denominator of $s_{hug'c}(z)$ and f , g , h into the coefficients of the numerator of $Y_{hug'}(z)$, we get that the condition is

$$cond = \frac{Y_0^2((b_1 + 1)z_0^2 - 1)}{2} < 0,$$

it follows that the condition **L2** is satisfied if and only if $-1/\sqrt{b_1 + 1} < z < 1/\sqrt{b_1 + 1}$.

2 Lax's inequalities in the wave manifold

The Lax's inequalities for shocks are used to select shock (entropy condition) and used to prove uniqueness in the solution.

For a 2 system of equations (1.1), we have a pair of inequalities associated to a 1-shock and another pair of inequalities associated to a 2-shock.

In the Lax's theory, the system is strictly hyperbolic with two different eigenvalues $\lambda_1(W) < \lambda_2(W)$. For regions for which the solution is continuous, we can define the i -characteristic on the plane xt , for $i = 1, 2$, solving:

$$\frac{dx}{dt} = \lambda_i(W). \quad (2.1)$$

For a shock between a state $W^- = (u^-, v^-)$ to $W^+ = (u^+, v^+)$, with shock speed $s(W^-, W^+)$, the 1-shock satisfies the inequalities given by:

$$s(W^-, W^+) < \lambda_1(W^-) \quad \text{and} \quad \lambda_1(W^+) < s(W^-, W^+) < \lambda_2(W^+). \quad (2.2)$$

The condition (2.2) states that the 1-characteristic wave, on the plane xt , (of each side of the shock) enter in the shock wave (with slope s).

The 2-shock satisfies the inequalities given by:

$$s(W^-, W^+) > \lambda_2(W^+) \quad \text{and} \quad \lambda_1(W^-) < s(W^-, W^+) < \lambda_2(W^-). \quad (2.3)$$

The condition (2.3) states that the 2-characteristic wave, on the plane xt , (of each side of the shock) enter in the shock wave (with slope s).

Here, we describe the Lax inequalities in the wave manifold.

For a state $\mathcal{U} \in \mathcal{W}$, using the Hugoniot', we obtain the projections $\mathcal{U}'_s \in \mathcal{C}_s$ and $\mathcal{U}'_f \in \mathcal{C}_f$, using Eq. (6.1). So, we have that the eigenvalue associated to λ_1 in the wave manifold is λ_s and the eigenvalue associated to λ_2 in the wave manifold is λ_f . We consider another $\tilde{\mathcal{U}} \in sh(\mathcal{U})$, whose projections in \mathcal{C}_s and \mathcal{C}_f are, respectively, $\tilde{\mathcal{U}}'_s$ and $\tilde{\mathcal{U}}'_f$.

Using the previous analysis, the 1-shock in the wave manifold between the states $\mathcal{U} \in \mathcal{W}$ and $\tilde{\mathcal{U}} \in sh(\mathcal{U})$ becomes:

$$s(\tilde{\mathcal{U}}) \leq s(\mathcal{U}'_s) = \lambda_s(\mathcal{U}'_s) \quad \text{and} \quad \lambda_s(\tilde{\mathcal{U}}) = s(\tilde{\mathcal{U}}'_s) < s(\tilde{\mathcal{U}}) < s(\tilde{\mathcal{U}}'_f) = \lambda_f(\tilde{\mathcal{U}}'_f). \quad (2.4)$$

Here, we use that the shock speed s equals to the λ in \mathcal{C} .

The 2-shock in the wave manifold between the states $\mathcal{U} \in \mathcal{W}$ and $\tilde{\mathcal{U}} \in sh(\mathcal{U})$ becomes:

$$s(\tilde{\mathcal{U}}) < s(\mathcal{U}'_f) = \lambda_f(\tilde{\mathcal{U}}'_f) \quad \text{and} \quad \lambda_s(\mathcal{U}') = s(\mathcal{U}'_s) < s(\tilde{\mathcal{U}}) < s(\mathcal{U}'_f) = \lambda_f(\mathcal{U}'_f). \quad (2.5)$$

3 Choices

3.1 Choice 1

This paper, as many previous ones, studies systems of two conservation laws 1.1, *i.e.*, system

$$W_t + F(W)_x = 0,$$

with $F = (f, g)$ where $f(u, v) = v^2/2 + (b_1 + 1)u^2/2 + a_1u + a_2v$ and $g(u, v) = uv + a_3u + a_4v$. Actually, here we are considering the so called symmetric case ($b_2 = 0$).

Why these particular f and g ?

In [9], the above equation was considered with the hypothesis that DF was hyperbolic (distinct eigenvalues) everywhere except at $(0, 0)$ where $DF(0, 0) = I_{2 \times 2}$, *i.e.*, $(0, 0)$ is an umbilic point. This led to the study of F quadratic and it was shown that it is sufficient to consider $F = grad(C)$ with $C = au^3/3 + buv + uv^2$.

In [8], it was started the study of $F = grad(C) +$ linear terms, in such a way that F is no longer a gradient. The addition of linear terms replaced the umbilic point by an elliptic region. Before adding linear terms, a simple change of coordinates was done and C became $uv^2/2 + [(b_1 + 1)u^3]/6 - b_2v^3/6$. The reason for this change of coordinates was to simplify the differential equation of the eigenspaces of DF . Subsequent papers kept this choice of F .

3.2 Choice 2

Where did the coordinates t and z came from?

In [7] were introduced coordinates $\tilde{U}, \tilde{V}, X, Y, Z$. In these coordinates, the wave manifold was given by the pair of equations $(1 - Z^2)\tilde{V} - Z\tilde{U} + c = 0; Y = ZX$. Both natural choices (\tilde{U}, Z, X) and (\tilde{V}, Z, X) of coordinates for the wave manifold were used.

In this paper, we are treating case IV in the classification of [9]. In this case the secondary bifurcation is contained in plane $Z = 0$, in order to stay away from it we use $z = \frac{1}{Z}$. For technical reasons, we replace \tilde{V} by $V_1 = \tilde{V} + a_2$. So, the equations of the wave manifold become $(z^2 - 1)V_1 - z\tilde{U} + c = 0; X = zY$.

We would like to use coordinates which would be valid for the whole wave manifold, except the plane $z = \infty$ which is formed by Hugoniot curve of points in the secondary bifurcation.

We begin writing the equation of characteristic surface \mathcal{C} , $(z^2 - 1)V_1 - z\tilde{U} + c = 0$, in (\tilde{U}, V_1, z) -space and add the coordinate Y .

We recall that \mathcal{C} is a ruled surface, *i.e.*, for fixed z we have a horizontal line in (\tilde{U}, V_1, z) -space. In the (\tilde{U}, V_1) -plane, the line is in the direction of vector $(z^2 - 1, z)$. We also know that coincidence curve is the singular set of the projection $(\tilde{U}, V_1, z) \mapsto (\tilde{U}, V_1, 0)$ restricted to \mathcal{C} . Putting $h(\tilde{U}, V_1, z) = (z^2 - 1)V_1 - z\tilde{U} + c$, a parametrization of the coincidence curve is obtained solving the linear system

$$\begin{cases} h(\tilde{U}, V_1, z) = 0 \\ \frac{dh(\tilde{U}, V_1, z)}{dz} = 0, \end{cases} \quad (3.1)$$

as a system in \tilde{U}, V_1 , obtaining $\tilde{U} = (2cz)/(z^2 + 1)$ and $V_1 = c/(z^2 + 1)$. In order to introduce the coordinate t , we take the rules of surface \mathcal{C} starting at the coincidence curve. For fixed z the coordinate t measures how much the point moves away from the coincidence curve in the direction of the rules, *i.e.*, $\tilde{U} = (2cz)/(z^2 + 1) + t(z^2 - 1)$ and $V_1 = c/(z^2 + 1) + tz$.

Acknowledgements

The authors are grateful to Bradley Plohr for many enlightening discussions, mainly concerning the use of lax conditions and the use of the ELI software to check our results.

References

- [1] A. V. Azevedo, C. S. Eschenazi, D. Marchesin, and C. F. Palmeira, *Topological resolution of riemann problems for pairs of conservation laws*, Quarterly of Applied Mathematics **68** (2010), 375–393.
- [2] J. Bastos-Gonçalves and H. Reis, *The Geometry of Quadratic 2×2 Systems of Conservation Laws*, Acta Applicandae Mathematicae **88** (2005), 269–329.
- [3] C. S. Eschenazi and C. F. B. Palmeira, *The structure of composite rarefaction-shock foliations for quadratic systems of conservation laws*, Matemática Contemporânea **22** (2002), 113–140.
- [4] ———, *Intersections of Hugoniot curves with the sonic surface in the wave manifold*, Bulletin of the Brazilian Mathematical Society, New Series **44(2)** (2013), 255–272.
- [5] E. Isaacson, D. Marchesin, C. F. Palmeira, and B. Plohr, *A global formalism for nonlinear waves in conservation laws*, Comm. Math. Phys. **146** (1992), 505–552.
- [6] E. P. López-Bambarén, *Choques não-locais na variedade de ondas em sistemas quadráticos de duas leis de conservação*, Dep. de Matemática, Universidade Federal de Minas Gerais, Brasil, Doctoral Thesis, in Portuguese, (2020).
- [7] D. Marchesin and C. F. B. Palmeira, *Topology of elementary waves for mixed-type systems of conservation laws*, Journal of Dynamics and Differential Equations **6** (1994), no. 3, 421–440.
- [8] C. F. B. Palmeira, *Line Fields Defined by Eigenspaces of Derivatives of Maps from the Plane to Itself*, Proceedings of the VIth International Conference of Differential Geometry, Santiago de Compostela, Spain, (1988), 177–205.
- [9] D. Schaeffer and M. Shearer, *The classification of 2×2 systems of non-strictly hyperbolic conservation laws, with application to oil recovery, with appendix by D. Marchesin, P.J. Paes Leme, D.G. Schaeffer, M. Shearer*, Comm. Pure Appl. Math. **40** (1987), 141–178.
- [10] J. Smoller, *Shock Waves and Reaction–Diffusion Equations*, 2nd. Ed, Springer-Verlag New York, 1994.